

1 **Protective activity of mRNA vaccines against ancestral and variant SARS-CoV-2**
2 **strains**

3
4 Baoling Ying^{1*}, Bradley Whitener^{1*}, Laura A. VanBlargan^{*1}, Ahmed O. Hassan^{*1}, Swathi
5 Shrihari¹, Chieh-Yu Liang^{1,6}, Courtney E. Karl^{1,7}, Samantha Mackin^{1,6}, Rita E. Chen^{1,6}, Natasha
6 M. Kafai^{1,6}, Samuel H. Wilks², Derek J. Smith², Juan Manuel Carreño³, Gagandeep Singh³,
7 Florian Krammer³, Andrea Carfi⁴, Sayda Elbashir⁴, Darin K. Edwards⁴, Larissa B. Thackray^{1¶},
8 and Michael S. Diamond^{1,5,6,7 ¶‡}

9
10 ¹Department of Medicine, Washington University School of Medicine, St. Louis, MO 63110, USA

11 ²Center for Pathogen Evolution, Department of Zoology, University of Cambridge, Cambridge UK.

12 ³Department of Microbiology, Icahn School of Medicine at Mount Sinai, New York, NY, USA.

13 ⁴Moderna, Inc., Cambridge MA, USA

14 ⁵Department of Pathology & Immunology, Washington University School of Medicine, St. Louis, MO, USA

15 ⁶Department of Molecular Microbiology, Washington University School of Medicine, St. Louis, MO, USA

16 ⁷The Andrew M. and Jane M. Bursky Center for Human Immunology and Immunotherapy Programs,
17 Washington University School of Medicine. St. Louis, MO, USA

18
19 *Equal contributors

20 ¶ Corresponding authors: Larissa B. Thackray, Ph.D. (lthackray@wustl.edu) and Michael S.

21 Diamond, M.D., Ph.D. (diamond@wusm.wustl.edu)

22 ‡ Lead Contact: Michael S. Diamond, M.D., Ph.D.

23

24 **SUMMARY (150 words)**

25 Although mRNA vaccines prevent COVID-19, variants jeopardize their efficacy as
26 immunity wanes. Here, we assessed the immunogenicity and protective activity of historical
27 (mRNA-1273, designed for Wuhan-1 spike) or modified (mRNA-1273.351, designed for B.1.351
28 spike) preclinical Moderna mRNA vaccines in 129S2 and K18-hACE2 mice. Immunization with
29 high or low dose formulations of mRNA vaccines induced neutralizing antibodies in serum
30 against ancestral SARS-CoV-2 and several variants, although levels were lower particularly
31 against the B.1.617.2 (Delta) virus. Protection against weight loss and lung pathology was
32 observed with all high-dose vaccines against all viruses. Nonetheless, low-dose formulations of
33 the vaccines, which produced lower magnitude antibody and T cell responses, and serve as a
34 possible model for waning immunity, showed breakthrough lung infection and pneumonia with
35 B.1.617.2. Thus, as levels of immunity induced by mRNA vaccines decline, breakthrough
36 infection and disease likely will occur with some SARS-CoV-2 variants, suggesting a need for
37 additional booster regimens.

38 INTRODUCTION

39 Severe acute respiratory syndrome coronavirus 2 (SARS-CoV-2) is the cause of the
40 Coronavirus Disease 2019 (COVID-19) syndrome. More than 211 million infections and 4.4
41 million deaths have been recorded worldwide (<https://covid19.who.int>) since the start of the
42 pandemic. The extensive morbidity and mortality associated with the COVID-19 pandemic made
43 the development of SARS-CoV-2 vaccines a global health priority. In a short period of less than
44 one year, several highly effective vaccines targeting the SARS-CoV-2 spike protein
45 encompassing multiple platforms (lipid nanoparticle encapsulated mRNA, inactivated virion, or
46 viral-vectored vaccine platforms (Graham, 2020)) gained Emergency Use Authorization or Food
47 and Drug Administration approval and were deployed with hundreds of millions of doses given
48 worldwide (<https://covid19.who.int>). The currently used vaccines all were designed against the
49 spike protein of strains that were circulating early in the pandemic. In localities with high rates of
50 vaccination, markedly reduced numbers of infections, hospitalizations, and deaths were initially
51 observed.

52 Despite the success of COVID-19 vaccines and their potential for curtailing the
53 pandemic, the continued evolution of more transmissible SARS-CoV-2 variants of concern
54 (VOC) including B.1.1.7 (Alpha), B.1.351 (Beta), B.1.1.28 (Gamma), and B.1.617.2 (Delta) with
55 substitutions in the spike protein jeopardizes the efficacy of vaccination campaigns (Krause et
56 al., 2021). Experiments in cell culture suggest that neutralization by vaccine-induced sera is
57 diminished against variants expressing mutations in the spike gene at positions L452, E484,
58 and elsewhere (Chen et al., 2021b; McCallum et al., 2021a; Tada et al., 2021; Wang et al.,
59 2021a; Wang et al., 2021b; Wibmer et al., 2021). Moreover, viral-vectored (ChAdOx1 nCoV-19
60 and Ad26.CoV2) and protein nanoparticle (NVX-CoV2373)-based vaccines showed reduced
61 activity (10 to 60%) against symptomatic infection caused by the B.1.351 variant in clinical trials
62 in humans (Madhi et al., 2021; Sadoff et al., 2021; Shinde et al., 2021), whereas mRNA-based

63 vaccines (e.g., BNT162b2) retained substantial (~75%) efficacy against the B.1.351 variant in
64 humans with almost complete protection against severe disease (Abu-Raddad et al., 2021).

65 Immunization of humans with two 100 µg doses of the lipid nanoparticle-encapsulated
66 mRNA-1273 vaccine encoding a proline-stabilized full-length SARS-CoV-2 spike glycoprotein
67 corresponding to the historical Wuhan-Hu-1 virus conferred 94% efficacy against symptomatic
68 COVID-19 in clinical trials performed in the United States (Baden et al., 2021). More recent data
69 in non-human primates shows that vaccination with two doses of mRNA-1273 results in an
70 effective immune response that controls upper and lower respiratory tract infection after
71 challenge with the SARS-CoV-2 B.1.351 viral variant (Corbett et al., 2021). As an alternative
72 approach, several manufacturers have designed modified vaccines that target specific VOC
73 including B.1.351 for possible immunization or boosting. Indeed, a mRNA-1273.351 vaccine
74 recently was generated, which encodes a proline stabilized full-length SARS-CoV-2 spike
75 glycoprotein from the B.1.351 virus. Here, we evaluated the immunogenicity and protective
76 activity of lipid-encapsulated mRNA-1273 and mRNA-1273.351 Moderna vaccines in the
77 context of challenge of wild-type 129S2 and human ACE2 (hACE2) transgenic (K18-hACE2)
78 mice with historical and emerging SARS-CoV-2 strains including several key VOC.

79 RESULTS

80 **Immunogenicity of mRNA vaccines in 129S2 mice.** We first tested preclinical
81 versions of the Moderna mRNA-1273 and mRNA-1273.351 vaccines encoding sequenced-
82 optimized prefusion-stabilized spike proteins of Wuhan-1 and B.1.351, respectively, in
83 immunocompetent 129S2 mice. These animals are permissive to infection by some SARS-CoV-
84 2 variants (e.g., B.1.1.7, B.1.1.28, and B.1.351) or mouse-adapted strains (Chen et al., 2021a;
85 Gu et al., 2020; Rathnasinghe et al., 2021) that encode an N501Y mutation, which enables
86 engagement of endogenous murine ACE2 (Liu et al., 2021b). Infection of 129S2 mice with
87 SARS-CoV-2 results in mild to moderate lung infection and clinical disease with subsequent
88 recovery (Chen et al., 2021a; Rathnasinghe et al., 2021). To assess the immunogenicity of the
89 vaccines, groups of 7 to 9-week-old female 129S2 mice were immunized and boosted three
90 weeks later by an intramuscular route with 5 µg (high) or 0.25 µg (low) doses of mRNA-1273,
91 mRNA-1273.351, mRNA-1273.211 (1:1 mixture [total 5 or 0.25 µg] of mRNA-1273 and mRNA-
92 1273.351), or a control non-coding mRNA (**Fig 1A**); we included the mRNA-1273.211 mixture
93 since it is being tested in humans (NCT04927065 (Wu et al., 2021)). Serum samples were
94 collected three weeks after boosting, and IgG responses against recombinant spike proteins of
95 ancestral (Wuhan-1) or variant (B.1.1.7, B.1.351, or B.1.617.2) viruses (Amanat et al., 2021)
96 were evaluated by ELISA (**Fig 1B**). As expected, the control mRNA did not generate spike-
97 specific IgG (values below the limit of detection), whereas antibody responses against the spike
98 proteins from all other mRNA vaccines were robust. For the 5 µg dose, mean endpoint titers of
99 serum ranged from 619,650 to 1,503,560 against the different spike proteins with little variation
100 between the mRNA vaccines. For the 0.25 µg dose, approximately 5-fold lower serum IgG
101 responses were observed with mean endpoint titers ranging from 126,900 to 382,725, again
102 with little difference between the mRNA vaccines. The responses trended slightly higher against
103 the ancestral spike protein and lower against the B.1.617.2 spike protein although most of these

104 differences did not attain statistical significance. Overall, both doses and all spike-based vaccine
105 formulations generated strong anti-spike protein IgG responses in 129S2 mice.

106 We characterized serum antibody responses functionally by assaying inhibition of
107 SARS-CoV-2 infectivity using a focus-reduction neutralization test (FRNT) (Case et al., 2020b).
108 We tested a panel of sera from each group of vaccinated mice against several fully-infectious
109 SARS-CoV-2 strains including an ancestral Washington strain with a single D614G substitution
110 (WA1/2020 D614G) or one with both D614G and N501Y substitutions (WA1/2020
111 D614G/N501Y), a B.1.1.7 isolate encoding an E484K mutation (B.1.1.7/E484K), a B.1.351
112 isolate, and a B.1.617.2 isolate (**Fig 1C-L**). Due to the limited amount of sera recovered from
113 live animals, we started dilutions at 1/180. As expected, serum from all control mRNA-
114 immunized mice did not inhibit infection of the SARS-CoV-2 strains (**Fig 1C-L**). For the 5 μ g
115 dose, all three spike gene vaccines (mRNA-1273, mRNA-1273.351, and mRNA-1273.211)
116 induced robust serum neutralizing antibody responses (**Fig 1C-G**). In general, these titers were
117 similar with the exception of ~4-fold lower geometric mean titers (GMTs) against WA1/2020
118 D614G and ~2-fold higher GMTs against B.1.351 induced by mRNA-1273.351 compared to the
119 mRNA-1273 and mRNA-1273.211 vaccines. Lower neutralizing responses (~4- to 5-fold) were
120 seen against the B.1.617.2 strain by all three mRNA vaccines (**Fig 1G**). For the 0.25 μ g vaccine
121 dose, we observed ~10-fold lower levels of serum neutralizing activity against each of the
122 viruses (**Fig 1H-L**) and noted the following trends: (a) the mRNA-1273.351 vaccine induced
123 lower levels of neutralizing antibody against WA1/2020 D614G and WA1/2020 D614G/N501Y
124 than the mRNA-1273 vaccine (**Fig 1H-I**); (b) the mRNA-1273.211 mixture generally induced
125 neutralizing antibodies that were equivalent to one of the two vaccine components; (c) serum
126 from mRNA-1273-vaccinated mice showed smaller reductions in neutralization against B.1.351
127 than anticipated based on prior studies in humans and C57BL6 mice (Chen et al., 2021b; Wang
128 et al., 2021a) (**Fig 1J**); (d) serum from mRNA-1273.351-vaccinated mice trended toward higher

129 neutralization against B.1.351; and (e) serum neutralizing antibody levels from all vaccinated
130 mice were lower against B.1.617.2 than other strains, although responses from animals
131 administered mRNA-1273 were somewhat higher (**Fig 1L**). Overall, these differences were
132 visualized best in a comparative analysis of the inhibitory activity of each serum sample for the 5
133 μg (**Fig S1A-C**) and 0.25 μg (**Fig S1D-F**) doses.

134 Using the neutralization data from mRNA vaccinated 129S2 mice, we created antigenic
135 maps to visualize the relationships between the WA1/2020 D614G, WA1/2020 D614G/N501Y,
136 B.1.1.7/E484K, B.1.351, and B.1.617.2 SARS-CoV-2 strains (**Fig 1M-N**). Neutralization titers
137 obtained after 5 or 0.25 μg dosing with mRNA-1273 and mRNA-1273.351 vaccines were used
138 to position the serum relative to each virus using antigenic cartography (a modification of
139 multidimensional scaling for binding assay data), such that higher neutralization titers are
140 represented by shorter distances between serum and the virus. Each gridline, or antigenic unit,
141 of the map corresponds to a 2-fold difference in neutralization titer of a given virus. Three
142 antigen clusters were observed: (a) WA1/2020 D614G and WA1/2020 D614G/N501Y grouped
143 together; (b) viruses containing E484K mutations (B.1.1.7/E484K and B.1.351) had a similar
144 antigenic position; and (c) B.1.617.2 was the most distant antigenically, which is consistent with
145 the lower levels of serum neutralization induced by all of the mRNA vaccines against this VOC.

146 **Protection by mRNA vaccines in 129S2 mice.** We tested the protective activity of the
147 different mRNA vaccines in 129S2 mice. Three weeks after boosting, mice were challenged via
148 an intranasal route with WA1/2020 N501Y/D614G, B.1.1.7/E484K, or B.1.351. The WA1/2020
149 D614G and B.1.617.2 viruses were not used for challenge in this model since they lack the
150 mouse-adapting N501Y substitution and cannot infect conventional laboratory mice (Gu et al.,
151 2020). Compared to the control mRNA vaccine, the 5 μg or 0.25 μg doses of mRNA-1273,
152 mRNA-1273.351, or mRNA-1273.211 vaccines all prevented weight loss between 2 and 4 dpi,

153 although protection was not statistically significant for some groups immunized with the mRNA-
154 1273 vaccine and challenged with B.1.351 or B.1.1.7/E484K viruses (**Fig 2A-B**).

155 At 4 days post-infection (dpi), mice were euthanized, and nasal washes, lungs, and
156 spleen were collected for viral burden analysis. In the nasal washes or lungs from control
157 mRNA-vaccinated 129S2 mice, high levels ($\sim 10^7$ copies of *N* per mL or mg) of viral RNA were
158 measured after challenge with WA1/2020 N501Y/D614G, B.1.1.7/E484K, or B.1.351 (**Fig 2C-**
159 **D**). Lower levels of SARS-CoV-2 RNA ($\sim 10^2$ to 10^4 copies of *N* per mg) were measured in the
160 spleen (**Fig S2A**). In general, the mRNA-1273, mRNA-1273.351, and the mRNA-1273.211
161 vaccines conferred robust protection against infection in nasal washes, lungs, and spleens by
162 the challenge SARS-CoV-2 strains, although some breakthrough was noted. After the 5 μ g dose
163 immunization with mRNA-1273, moderate B.1.1.7/E484K infection was detected in nasal
164 washes in 5 of 8 mice, although viral RNA was absent from the lungs. Some (3 of 8) mice
165 immunized with the mRNA-1273.211 mixture also showed breakthrough in the lungs, albeit at
166 greater than 100-fold lower levels than the control vaccine. In comparison, the 5 μ g dose of
167 mRNA-1273.351 was protective in the nasal wash and lungs against all viruses, with little, if
168 any, viral RNA measured.

169 As expected, the 0.25 μ g dose of the mRNA vaccines showed less protective efficacy
170 against SARS-CoV-2 challenge. With few exceptions (2 mice, mRNA-1273.351), the protection
171 conferred by the 0.25 μ g dose against WA1/2020 N501Y/D614G and B.1.1.7/E484K challenge
172 was strong in the nasal washes at 4 dpi (**Fig 2C**). In comparison, after B.1.351 challenge, 8 of 8
173 mice immunized with mRNA-1273 showed viral RNA in nasal washes, with 3 of 8 showing
174 levels that approached those seen in control-vaccinated mice. Greater protection was generated
175 against B.1.351 by mRNA-1273.351 or the mRNA-1273.211 mixture vaccine, although
176 breakthrough infections were detected. In the lungs, strong protection against infection with
177 WA1/2020 N501Y/D614G was generated by all three spike mRNA vaccines (**Fig 2D**). However,

178 some infection was seen after B.1.1.7/E484K or B.1.351 challenge. For example, 6 of 8 mice
179 immunized with mRNA-1273 had moderate to high levels of B.1.351 viral RNA in their lungs at 4
180 dpi.

181 We assessed for correlations between vaccine-induced neutralizing antibody titers and
182 protection against SARS-CoV-2 infection in the lung after virus challenge. Serum levels of
183 neutralizing antibody were associated inversely with SARS-CoV-2 RNA levels in the lung (**Fig**
184 **2E**) with a minimum neutralizing titer of approximately 5,000 required to prevent infection in the
185 lung at 4 dpi. Most of the breakthrough infections occurred with the B.1.351 challenge at the
186 0.25 µg dose of vaccines. For reasons that remains unclear, the threshold for complete
187 protection in the lung after challenge with WA1/2020 N501Y/D614G was lower (2 to 7-fold) than
188 against the other viruses. Moreover, when we compared body weight change at 4 dpi with
189 neutralizing titers, only animals challenged with B.1.351 showed a linear correlation (**Fig S2B**),
190 possibly because of the greater number of breakthrough infections in this group.

191 We also assessed the effect of the mRNA vaccines on lung disease at 4 dpi in 129S2
192 mice. For these studies, we analyzed lung sections from the group of mice that received the
193 lower 0.25 µg vaccine dose and the B.1.351 challenge virus, as this combination resulted in the
194 greatest number of breakthrough infections. As expected, mice immunized with the control
195 mRNA vaccine and challenged with B.1.351 developed mild pneumonia characterized by
196 immune cell accumulation in perivascular and alveolar locations, vascular congestion, and
197 interstitial edema. In contrast, animals immunized with mRNA-1273, mRNA-1273.351, or
198 mRNA-1273.211 vaccines did not show these pathological changes (**Fig 3**). Thus, immunization
199 with even the low dose of the mRNA vaccines was sufficient to mitigate SARS-CoV-2-induced
200 lung injury in immunocompetent 129S2 mice challenged with some VOC.

201 **Immunogenicity of mRNA vaccines in K18-hACE2 transgenic mice.** We next
202 evaluated the mRNA-1273 and mRNA-1273.351 vaccines in K18-hACE2 transgenic mice,

203 which sustain higher levels of infection and disease after intranasal inoculation by many SARS-
204 CoV-2 strains (Winkler et al., 2020) including isolates containing or lacking mouse-adapting
205 mutations (e.g., N501Y) (Chen et al., 2021a). Due to a limited availability of K18-hACE2 mice
206 and the need to test two control viruses (WA1/2021 D614G and WA1/2021 D614G/N501Y), we
207 tested mRNA-1273 and mRNA-1273.351 but not the mRNA-1273.211 mixture vaccine. Groups
208 of 7-week-old female K18-hACE2 mice were immunized and boosted three weeks later by
209 intramuscular route with 5 or 0.25 µg doses of mRNA-1273, mRNA-1273.351, or control mRNA
210 vaccine (**Fig 4A**). Serum samples were collected three weeks after boosting, and IgG
211 responses against recombinant spike proteins (Wuhan-1, B.1.1.7, B.1.351, or B.1.617.2) were
212 evaluated by ELISA (**Fig 4B**). Antibody responses against the different spike proteins were
213 robust although slightly lower (~2 to 3-fold) than that seen in 129S2 mice (**Fig 1B**). Serum mean
214 endpoint IgG titers ranged from 218,700 to 1,601,425 against the different spike proteins with
215 little variation observed with the 5 µg doses of different mRNA vaccines. For the 0.25 µg dose,
216 lower (~6 to 10-fold) IgG titers were measured (24,300 to 101,250) with little difference between
217 the mRNA-1273 and mRNA-1273.351 vaccines. Although the IgG levels against the B.1.617.2
218 spike protein were reduced slightly compared to the other SARS-CoV-2 spike proteins, in
219 general, robust antibody responses were detected in K18-hACE2 mice.

220 We performed FRNTs to assess the neutralizing activity of pre-challenge serum against
221 WA1/2020 D614G, WA1/2020 D614G/N501Y, B.1.1.7/E484K, B.1.351, and B.1.617.2 SARS-
222 CoV-2 strains. Because of the limited amount of sera recovered from K18-hACE2 mice, we
223 initially started dilutions at 1/180. As expected, serum from all control mRNA-immunized mice
224 did not inhibit infection of the SARS-CoV-2 strains (**Fig 4C-L**). In general, neutralizing antibody
225 titers induced by 5 or 0.25 µg mRNA vaccine dosing trended lower (~ 3 to 6-fold) in immunized
226 K18-hACE2 than from 129S2 mice. For the 5 µg dose, while both mRNA-1273 and mRNA-
227 1273.351 vaccines induced robust serum neutralizing antibody responses, we observed the

228 following (**Fig 4C-G and Fig S3**): (a) the mRNA-1273.351 vaccine induced lower levels of
229 neutralizing antibody against WA1/2020 D614G and WA1/2020 D614G/N501Y than the mRNA-
230 1273 vaccine (**Fig 4C and D**); (b) a reciprocal pattern was observed against viruses containing
231 E484K mutations. The mRNA-1273.351 vaccine induced higher levels of neutralizing antibody
232 against B.1.1.7/E484K and B.1.351 than the mRNA-1273 vaccine (**Fig 4E and F**); and (c) no
233 differences in neutralizing activity were observed with the mRNA-1273 and mRNA-1273.351
234 vaccines against the B.1.617.2 strain. Although responses were elevated, they were lower than
235 against other strains (**Fig 4G**). Similar patterns were observed for the 0.25 μ g dose (**Fig 4H-L**),
236 although ~10-fold lower levels of neutralizing activity were induced by each vaccine against
237 each of the viruses. Because of this, we started our dilution series at 1/60 for sera derived from
238 animals immunized with the 0.25 μ g dose of mRNA vaccines. In general, the pattern of
239 neutralization paralleled results with the higher dose, with the mRNA-1273 vaccine performing
240 better against historical WA1/2020 viruses and the mRNA-1273.351 vaccine showing greater
241 inhibitory titers against B.1.351 (**Fig 4H, I and K**). However, serum from mice vaccinated with
242 mRNA-1273 or mRNA-1273.351 vaccines neutralized B.1.617.2 less efficiently (**Fig 4L**), with
243 several data points at the limit of detection (1/60: mRNA-1273, 4 of 24; mRNA-1273.351, 9 of
244 24) and responses induced by mRNA-1273 trending higher. A comparative analysis of the
245 inhibitory activity of each serum sample for the 5 μ g (**Fig S3A-B**) and 0.25 μ g (**Fig SC-D**) doses
246 visually showed these differences, as serum induced by the mRNA-1273 vaccine consistently
247 showed less neutralizing activity against B.1.1.7/E484K, B.1.351, and B.1.617.2, whereas
248 serum from mRNA-1273.351-vaccinated mice had greater inhibitory activity against B.1.351 and
249 B.1.1.7/E484K.

250 We used the neutralization data from mRNA-vaccinated K18-hACE2 mice to generate
251 maps defining the antigenic relationships between WA1/2020 D614G, WA1/2020
252 D614G/N501Y, B.1.1.7/E484K, B.1.351, and B.1.617.2 SARS-CoV-2 strains (**Fig 4M-N**). Serum

253 obtained after 5 or 0.25 µg dosing with mRNA-1273 or mRNA-1273.351 vaccines was analyzed
254 against the indicated viruses, and each antigenic unit corresponded to a 2-fold difference in
255 neutralization titer of a given virus. The results were remarkably similar to that seen with 129S2
256 vaccinated mice (**Fig 1M-N**): (a) WA1/2020 D614G and WA1/2020 D614G/N501Y grouped
257 together; (b) B.1.1.7/E484K and B.1.351 viruses, which contain E484K mutations, grouped near
258 each other; and (c) B.1.617.2 localized to a separate antigenic group.

259 We also examined T cell responses in mRNA-vaccinated K18-hACE2 mice two weeks
260 after boosting (**Fig 4A and M-Q**) using H-2^b restricted immunodominant peptides in the spike
261 protein for CD8⁺ and CD4⁺ T cells. After peptide stimulation *ex vivo* and staining for intracellular
262 IFN-γ production, we detected a robust CD8⁺ T cell (~2 to 4 percent positive) response in the
263 spleens of animals immunized with 5 µg of the mRNA-1273 or mRNA-1273.351 vaccines (**Fig**
264 **4O and P**). The response was approximately 10-fold lower in animals immunized with the lower
265 0.25 µg dose. While we also detected a spike protein-specific CD4⁺ T cell response after
266 immunization (~0.5 to 1.5 percent positive) with the 5 µg dose of mRNA-1273 or mRNA-
267 1273.351 vaccines, it was lower in magnitude (**Fig 4Q and R**). Moreover, the low 0.25 µg dose
268 mRNA-1273 or mRNA-1273.351 vaccines induced CD4⁺ T cell responses that were barely
269 greater than the control mRNA vaccine.

270 **Protection by mRNA vaccines in K18-hACE2 transgenic mice.** We next evaluated
271 the protective activity of the mRNA vaccines in K18-hACE2 mice. Three to four weeks after
272 boosting, mice were challenged via intranasal route with WA1/2020 D614G, WA1/2020
273 N501Y/D614G, B.1.1.7/E484K, B.1.351, or B.1.617.2 strains. Compared to the control mRNA
274 vaccine, the 5 µg and 0.25 µg doses of mRNA-1273 and mRNA-1273.351 vaccines all
275 prevented the weight loss occurring between 3 and 6 dpi (**Fig 5A-B**).

276 At 6 dpi, mice were euthanized, and nasal washes, lungs, and brains were collected for
277 viral burden analysis (**Fig 5C-D, and S4A**). In the nasal washes of control mRNA-vaccinated

278 K18-hACE2 mice, although some variability was observed, moderate levels ($\sim 10^5$ copies of *N*
279 per mL) of viral RNA were measured after challenge with WA1/2020 D614G, WA1/2020
280 N501Y/D614G, B.1.1.7/E484K, B.1.351, or B.1.617.2 strains (**Fig 5C**). In comparison, in the
281 lungs of control mRNA-vaccinated K18-hACE2 mice, higher and more uniform levels ($\sim 10^7$
282 copies of *N* per mg) of viral RNA were detected after challenge with all SARS-CoV-2 strains
283 (**Fig 5D**). The brains of control RNA-vaccinated K18-hACE2 mice showed some variability, as
284 seen previously (Winkler et al., 2020), with many but not all animals showing substantial
285 infection (10^8 copies of *N* per mL) (**Fig S4A**). The high 5 μ g dose of mRNA-1273 or mRNA-
286 1273.351 vaccines protected against infection in nasal washes, lung, and brain, with virtually no
287 viral breakthrough regardless of the challenge strain. After the 0.25 μ g dose immunization with
288 mRNA-1273, a loss of protection against infection in the nasal washes (3 of 7 mice) and lungs
289 (4 of 4 mice) was observed after challenge with B.1.351 and in the lungs only after challenge
290 with B.1.1.7/E484K (6 of 7 mice) or B.1.617.2 (8 of 8 mice) viruses. After the 0.25 μ g dose
291 immunization with mRNA-1273.351, incomplete protection against infection in the nasal
292 washes, lungs, and brain also was observed after challenge with WA1/2020 D614G (6, 7, and 4
293 of 8 mice, respectively), WA1/2020 D614G/N501Y (8, 4, and 6 of 8 mice, respectively),
294 B.1.1.7/E484K (8, 6, and 3 of 8 mice, respectively), and B.1.617.2 (7, 8, and 5 of 8 mice,
295 respectively). The 0.25 μ g dose of the mRNA-1273.351 vaccine protected better against lung
296 and brain infection by the homologous B.1.351 virus than against other strains.

297 We explored whether vaccine-induced neutralizing antibody titers correlated with
298 protection after challenge with WA1/2020 D614G, WA1/2020 N501Y/D614G, B.1.1.7/E484K,
299 B.1.351, or B.1.617.2 viruses. In general, serum levels of neutralizing antibody inversely
300 correlated with viral RNA levels in the lung (**Fig 5E**) for all viruses, with more infection occurring
301 in animals with lower neutralization titers. However, for WA1/2020 D614G, WA1/2020
302 N501Y/D614G, B.1.1.7/E484K, and B.1.351, some of the animals with low neutralization titers

303 still were protected against infection in the lung. The correlation was most linear for B.1.617.2-
304 challenged animals, with a minimum neutralizing titer of approximately 2,000 required to
305 completely prevent infection at 6 dpi. Most of the breakthrough B.1.617.2 infections occurred
306 with the 0.25 μ g dose of mRNA vaccines. The threshold for complete protection in the lung after
307 virus challenge varied somewhat with lower levels required for WA1/2020 D614G and
308 WA1/2020 N501Y/D614G. When we compared body weight change in K18-hACE2 mice at 6
309 dpi with neutralizing titers, a linear relationship was observed with all challenge viruses except
310 B.1.351 (**Fig S4B**). The best correlation was seen after B.1.617.2 challenge, with greater weight
311 loss in mice immunized with the 0.25 μ g vaccine dose and having lower serum neutralizing
312 antibody titers.

313 Because a pro-inflammatory host response to SARS-CoV-2 infection can contribute to
314 pulmonary pathology and severe COVID-19, we assessed the ability of the mRNA vaccines to
315 suppress cytokine and chemokine levels in the lung after virus challenge (**Fig S5**). For these
316 studies, K18-hACE2 mice were immunized and boosted with 5 or 0.25 μ g of control, mRNA-
317 1273 or mRNA-1273.351 vaccines and then challenged with WA1/2020 N501Y/D614G,
318 B.1.351, or B.1.617.2. SARS-CoV-2 infection of control mRNA vaccinated K18-hACE2 mice
319 resulted in high levels of expression in lung homogenates of several pro-inflammatory cytokines
320 and chemokines including G-CSF, IFN γ , IL-1 β , IL-6, CXCL1, CXCL5, CXCL9, CXCL10, CCL2,
321 and CCL4. Pro-inflammatory cytokine and chemokines in the lung at 6 dpi generally were
322 decreased in all mice vaccinated with 5 μ g doses of mRNA-1273 or mRNA-1273.351 regardless
323 of the challenge virus (**Fig S5A and B**). While this pattern also trended for the 0.25 μ g dose of
324 both mRNA vaccines, some cytokines and chemokines (e.g., IL-1 β , IL-6, CXCL9, and CXCL10)
325 remained elevated especially after challenge with B.1.617.2 (**Fig S5C and D**).

326 We evaluated the ability of the mRNA-1273 and mRNA-1273.351 vaccines to prevent
327 disease in K18-hACE2 mice by performing histological analysis of lung tissues from immunized

328 animals that were challenged with WA1/2020 D614G, WA1/2020 N501Y/D614G,
329 B.1.1.7/E484K, B.1.351, or B.1.617.2. As expected, lung sections obtained at 6 dpi from mice
330 immunized with the control mRNA vaccine and challenged with any of the SARS-CoV-2 strains
331 showed severe pneumonia characterized by immune cell infiltration, alveolar space
332 consolidation, vascular congestion, and interstitial edema (**Fig 6 and 7**). In comparison, mice
333 immunized with the high 5 μ g dose of mRNA-1273 or mRNA-1273.351 did not develop lung
334 pathology, with histological findings similar to uninfected K18-hACE2 mice (**Fig 6**). Mice
335 immunized with the low 0.25 μ g dose of the mRNA vaccines however, showed different results
336 (**Fig 7**): (a) mice vaccinated with mRNA-1273 showed few, if any, pathological changes after
337 WA1/2020 D614G, WA1/2020 N501Y/D614G, or B.1.1.7/E484K challenge. Nonetheless, some
338 mRNA-1273 vaccinated mice challenged with B.1.351 showed pulmonary vascular congestion
339 and mild lung inflammation; (b) mice vaccinated with mRNA-1273.351 showed almost complete
340 protection after WA1/2020 D614G, B.1.1.7/E484K, or B.1.351 challenge, whereas scattered
341 inflammation and alveolar septal thickening was apparent in sections from some WA1/2020
342 N501Y/D614G challenged mice; (c) of note, lung sections from mice vaccinated with the lower
343 0.25 μ g dose mRNA-1273 or mRNA-1273.351 and challenged with B.1.617.2 showed evidence
344 of viral pneumonia with prominent foci of immune cells inflammation and airspace consolidation.
345 Thus, low doses immunization of original or modified mRNA vaccines do not fully protect K18-
346 hACE2 mice from challenge with B.1.617.2 and result in mild to moderate infection and lung
347 pathology.

348

349 **DISCUSSION**

350 Robust vaccine-induced immune responses and sustained protective activity against
351 emerging SARS-CoV-2 variants are needed to limit human disease and curtail the COVID-19
352 global pandemic. A concern in the field is whether immunity generated by vaccines will wane
353 sufficiently to lose activity against VOC with mutations or deletions in regions of the spike
354 protein recognized by neutralizing antibodies. In the current study, we evaluated the
355 immunogenicity and protective activity of high- and low-dose formulations of Moderna mRNA
356 vaccines targeting historical (mRNA-1273) or variant (mRNA-1273.351) strains. The low-dose
357 formulation study arm was designed to model waning immunity and assess for possible strain-
358 specific breakthrough infections. Indeed, the lower neutralizing antibody and T cell responses
359 measured with the 0.25 µg dose of mRNA-1273 or mRNA-1273.351 parallel those seen for
360 human antibody and T cell responses six months after a primary vaccination series with mRNA-
361 1273 (Mateus et al., 2021; Pegu et al., 2021).

362 Immunization of 129S2 or K18-hACE2 transgenic mice with mRNA-1273, mRNA-
363 1273.351, or the mRNA-1273.211 mixture induced neutralizing antibodies against spike in
364 serum against historical WA1/2020 and several key VOC. Challenge studies performed
365 approximately one month after the second vaccine dose showed robust protection against
366 weight loss and lung pathology with all high-dose vaccine formulations and infecting SARS-
367 CoV-2 strains. Nonetheless, the low-dose vaccine formulations showed evidence of viral
368 infection breakthrough and lung pathological changes consistent with pneumonia especially with
369 the B.1.617.2 strain, which correlated with lower strain-specific neutralizing antibody levels. In
370 general, variant-specific vaccine designs appeared to induce greater antibody responses and
371 confer more protection against homologous virus strains.

372 Our experiments expand upon a preliminary immunogenicity study, which showed that
373 vaccination of H-2^d BALB/c mice with mRNA-1273.351 resulted in high serum neutralizing
374 antibody titers against the B.1.351 lineage, whereas the mRNA-1273.211 vaccine induced

375 broad cross-variant neutralization (Wu et al., 2021). We performed experiments with two H-2^b
376 strains, 129S2 and K18-hACE2 C57BL/6, and observed some similarities and differences. In
377 K18-hACE2 mice, the mRNA-1273 vaccine, which encodes for the Wuhan-1 pre-fusion
378 stabilized spike, induced higher neutralizing titers against WA1/2020 strains but lower
379 responses against viruses containing E484K mutations in spike (B.1.1.7/E484K and B.1.351),
380 which agrees with recent immunization studies in NHPs (Corbett et al., 2021). Reciprocally, the
381 mRNA-1273.351 vaccine, which encodes for the B.1.351 pre-fusion stabilized spike, induced
382 higher neutralizing titers against B.1.1.7/E484K and B.1.351. In 129S2 mice, only the mRNA-
383 1273.351 vaccine induced a lower neutralizing response against WA1/2020 D614G, as the
384 remainder of the neutralizing antibody responses were largely equivalent between vaccines.
385 However, in both K18-hACE2 and 129S2 mice, the mRNA-1273 and mRNA-1273.351 vaccines
386 induced antibody responses that neutralized B.1.617.2 less efficiently than the other SARS-
387 CoV-2 strains. Analysis of serum antibodies and B cell repertoire against SARS-CoV-2 VOC
388 from ongoing human clinical trials comparing mRNA-1273 and mRNA-1273.351 vaccines will be
389 needed to corroborate our results obtained in small animal models. Indeed, the differences in
390 neutralizing antibody titers induced by mRNA-1273 against WA1/2020 D614G and B.1.351 in
391 mice were smaller in magnitude than that seen in humans one month after boosting, but similar
392 to that observed six months after boosting (Pegu et al., 2021).

393 While the high-dose vaccination regimen with mRNA-1273 and mRNA-1273.351
394 induced robust neutralizing antibody and T cell responses that conferred almost complete
395 protection against all strains, animals immunized with the low-dose scheme showed virological
396 and pathological breakthrough that varied with the vaccine formulation and challenge strain. The
397 low-dose vaccination approach we employed as a model for waning immunity resulted in
398 approximately 10 to 20-fold reduced peak neutralization titers and T cell responses compared to
399 the high-dose arm, which corresponds to the 90% loss observed 90 days after natural infection
400 or vaccination in humans (Ibarrondo et al., 2021). The greatest loss in antibody neutralization

401 (both 129S2 and K18-hACE2 mice) and protection (K18-hACE2 mice) consistently occurred
402 with the B.1.617.2 variant. In contrast, recent longitudinal studies in humans immunized with
403 mRNA-1273 showed lower levels of serum antibody recognition of B.1.351 than other VOC,
404 although live virus neutralization assays were not performed with B.1.617.2 (Pegu et al., 2021).
405 In our experiments with live virus, the loss of neutralizing activity was equivalent if not greater
406 for B.1.617.2 than B.1.351, as seen by others (Liu et al., 2021a). Based on sequence changes
407 in the spike protein (B.1.617.2: T19R, 156del, 157del, R158G, L452R, T478K, D614G, P681R,
408 and D950N; and B.1.351: D80A, D215G, 241del, 242del, 243del, K417N, E484K, N501Y,
409 D614G, A701V) and known binding sites in the receptor binding motif of neutralizing antibodies
410 (at residue E484), it is not apparent why neutralizing activity and protection in mice were less
411 against B.1.617.2 than B.1.351, although there was a direct correlation with levels of
412 neutralizing antibody and B.1.617.2 burden in the lung. Nonetheless, mutations in the B.1.617.2
413 alter key antigenic sites and can abrogate recognition by neutralizing antibodies (McCallum et
414 al., 2021b). Other possible explanations for the loss of potency of antibodies against B.1.617.2
415 include differential display of B.1.617.2 spike proteins on the surface of infected cells and
416 engagement of Fc effector functions (Ravetch et al., 2021; Winkler et al., 2021) or differential
417 ability of antibodies to block cell-to-cell spread in a strain-dependent manner (Kruglova et al.,
418 2021). Our observation of B.1.617.2 infection and lung disease in low-dose mRNA-vaccinated
419 K18-hACE2 mice as a model of waning immunity corresponds to descriptions of B.1.617.2
420 breakthrough infections in vaccinated humans in the United States, Israel, and elsewhere, some
421 of which have required hospitalization (Brown et al., 2021; Puranik et al., 2021).

422 Our studies in 129S2 and K18-hACE2 mice with parental and modified mRNA vaccines
423 show robust immunogenicity and protection against multiple SARS-CoV-2 strains when high-
424 dose immunization schemes are used, although some differences in immunity are seen with
425 particular vaccines against selected variants. While the lower dose of mRNA vaccines generally
426 protected against matched virus challenge infection (e.g., mRNA-1273 vaccination and

427 WA1/2020 challenge or mRNA-1273.351 vaccination and B.1.351 challenge), breakthrough
428 events were seen with some non-matched challenges (e.g., mRNA-1273 vaccination and
429 B.1.351 challenge or mRNA-1273.351 vaccination and WA1/2020 challenge). As the low dose
430 of mRNA-1273 and 1273.351 vaccines induced lower neutralizing titers and protected less
431 against challenge with the B.1.617.2 variant, higher titers will be needed to minimize B.1.617.2
432 infection, transmission, and disease. Although studies in humans are required, boosting with
433 historical or variant (e.g., mRNA encoding B.1.617.2 spike genes) vaccines might be required to
434 prevent breakthrough events as vaccine-induced immunity wanes.

435 **Limitations of study.** We note several limitations in our study. (1) The studies in 129S2
436 mice precluded challenge with B.1.617.2, as it does not infect murine cells because it lacks an
437 N501Y mutation. The generation of recombinant SARS-CoV-2 strains with spike genes
438 encoding B.1.617.2 and an N501Y mutation could overcome this limitation. (2) Female 129S2
439 and K18-hACE2 mice were used to allow for group caging of the large cohorts required for
440 these multi-arm vaccination studies. Follow-up experiments in male mice are needed to confirm
441 results are not sex-biased. (3) We used lower vaccine dosing as a model for waning immunity.
442 Studies that directly address durability of immune responses and protection are needed for
443 corroboration. (4) We used historical, variant, or mixed mRNA vaccine formulations with
444 homologous boosting schemes. Animals studies that test heterologous boosting (mRNA-1273
445 prime followed by mRNA-1273.351 boost) (Wu et al., 2021) also are needed to support clinical
446 trials. (5) Our studies focused on immunogenicity and protection in two strains of mice because
447 of the ability to set up large animal cohorts and the tools available for analysis. These results
448 require confirmation in other animal models of SARS-CoV-2 infection including hamsters and
449 non-human primates (Muñoz-Fontela et al., 2020). (6) We did not establish direct immunological
450 correlates of vaccine protection or failure for all vaccine and challenge strain pairs. While some
451 relationships were more predictive (e.g., low B.1.617.2 neutralizing titers and viral burden in the
452 lung), others were not.

453 **ACKNOWLEDGEMENTS**

454 This study was supported by grants and contracts from NIH (R01 AI157155,
455 HHSN75N93019C00074, T32 AI007172, NIAID Centers of Excellence for Influenza Research
456 and Response (CEIRR) contracts HHSN272201400008C and 75N93021C00014, and the
457 Collaborative Influenza Vaccine Innovation Centers (CIVIC) contract 75N93019C00051). This
458 work also was supported by the Alafi Neuroimaging Laboratory, the Hope Center for
459 Neurological Disorders, and NIH Shared Instrumentation Grant (S10 RR0227552). We thank
460 Marciela DeGrace for help in study design and funding support, Richard Webby, Mehul Suthar,
461 and Pei-Yong Shi for several of the viruses used in this study, Kristen Valentine and Sujan
462 Shresta for providing immunodominant T cell peptides in advance of publication, Barbara
463 Mühlemann for help with antigenic cartography, and Emma Winkler and Oleksandr Dmytrenko
464 for providing lung sections from naive mice. We acknowledge the Pulmonary Morphology Core
465 at Washington University School of Medicine for tissue sectioning and slide imaging.

466

467 **AUTHOR CONTRIBUTIONS**

468 L.A.V. and B.Y. performed and analyzed neutralization assays. B.Y., B.W., A.O.H.,
469 L.A.V., S.S., C.E.K., S.M., N.M.K., R.E.C., and L.B.T. performed mouse experiments. B.W.,
470 S.S., and C-Y.L. performed viral burden analyses. A.O.H. and B.Y. performed T cell analyses.
471 J.M.C., G.S., and F.K. performed and analyzed the ELISA experiments. S.H.W and D.J.S.
472 performed the antigenic cartography analysis. A.C., S.E., and D.E. provided the mRNA vaccines
473 and helped design experiments. M.S.D. obtained funding. L.B.T. and M.S.D. supervised the
474 research. M.S.D. and L.B.T. wrote the initial draft, with the other authors providing editorial
475 comments.

476

477 **COMPETING FINANCIAL INTERESTS**

478 M.S.D. is a consultant for Inbios, Vir Biotechnology, Fortress Biotech, and Carnival
479 Corporation, and on the Scientific Advisory Boards of Moderna and Immunome. The Diamond
480 laboratory has received unrelated funding support in sponsored research agreements from Vir
481 Biotechnology, Kaleido, Moderna, and Emergent BioSolutions. A.C., S.E., and D.K.E. are
482 employees of and shareholders in Moderna Inc. F.K. is a coinventor on a patent application for
483 serological assays and SARS-CoV-2 vaccines (international application numbers
484 PCT/US2021/31110 and 62/994,252).

485 **FIGURE LEGENDS**

486 **Figure 1. Immunogenicity analysis of mRNA vaccines in 129S2 mice.** Seven to
487 nine-week-old female 129S2 mice were immunized and boosted with 5 or 0.25 μg of mRNA
488 vaccines. **A.** Scheme of immunizations, blood draw, and virus challenge. **B.** Serum anti-spike
489 IgG responses at three weeks after booster immunization with mRNA vaccines (control (black
490 symbols), mRNA-1273 (red symbols), mRNA-1273.351 (blue symbols), and mRNA-1273.211
491 (green symbols) against indicated spike proteins (Wuhan-1, B.1.1.7, B.1.351, or B.1.617.2) ($n =$
492 3 (control vaccine) or 8 (spike vaccines), two independent experiments, boxes illustrate mean
493 values, dotted line shows the limit of detection (LOD); two-way ANOVA with Tukey's post-test: *,
494 $P < 0.05$). **C-L.** Serum neutralizing antibody responses three weeks after boosting as assessed
495 by FRNT (half-maximal reduction, FRNT₅₀ values) with WA1/2020 D614G (**C, H**), WA1/2020
496 D614G/N501Y (**D, I**), B.1.1.7/E484K (**E, J**), B.1.351 (**F, K**), or B.1.617.2 (**G, L**) in mice
497 immunized with 5 (**C-G**) or 0.25 (**H-L**) μg of control ($n = 6-10$), mRNA-1273, mRNA-1273.351, or
498 mRNA-1273.211 ($n = 12-21$) vaccines (two independent experiments, boxes illustrate geometric
499 mean values, dotted line shows LOD; one-way Kruskal-Wallis ANOVA with Dunn's post-test: *,
500 $P < 0.05$; **, $P < 0.01$; ***, $P < 0.001$; ****, $P < 0.0001$). **M-N.** Antigenic map of sera from 129S2
501 mice titrated against WA1/2020 D614G, WA1/2020 N501Y/D614G, B.1.1.7/E484K, B.1.351,
502 and B.1.617.2. The maps show sera from mice that received 5 μg (**M**) or 0.25 μg (**N**) doses,
503 respectively. Antigens (viruses) are shown as circles (WA1/2020 D614G: red, bigger circle,
504 WA1/2020 N501Y/D614G: red, smaller circle, B.1.1.7/E484K: turquoise, B.1.351: blue, and
505 B.1.617.2: orange) and sera as squares (blue for mRNA-1273.351-induced sera and red for
506 mRNA-1273-induced sera). The X and Y axes correspond to antigenic distance, with one grid
507 line corresponding to a two-fold serum dilution in the neutralization assay. The antigens and
508 sera are arranged on the map such that the distances between them best represent the
509 distances measured in the neutralization assay.

510 **Figure 2. Protection against SARS-CoV-2 infection after mRNA vaccination in**
511 **129S2 mice.** Seven to nine-week-old female 129S2 mice were immunized and boosted with 5
512 or 0.25 µg of mRNA vaccines (control (black symbols), mRNA-1273 (red symbols), mRNA-
513 1273.351 (blue symbols), and mRNA-1273.211 [mixture, green symbols]) as described in
514 **Figure 1A.** Three weeks after boosting, mice were challenged via intranasal inoculation with 10^5
515 focus-forming units (FFU) of WA1/2020 N501Y/D614G, B.1.1.7/E484K, or B.1.351. **A-B.** Body
516 weight change over time. Data shown is the mean \pm SEM (n = 6-9, two independent
517 experiments; one-way ANOVA of area under the curve from 2-4 dpi with Dunnett's post-test,
518 comparison to control immunized group: ns, not significant; $P > 0.05$; *, $P < 0.05$; **, $P < 0.01$;
519 ***, $P < 0.001$; **** $P < 0.0001$). **C-D.** Viral burden at 4 dpi in the nasal washes (**C**) and lungs (**D**)
520 as assessed by qRT-PCR of the *N* gene after challenge of immunized mice with the indicated
521 mRNA vaccines (n = 6-8, two independent experiments, boxes illustrate median values, dotted
522 line shows LOD; one-way Kruskal-Wallis ANOVA with Dunn's post-test, comparison among all
523 immunization groups: ns, not significant; $P > 0.05$; *, $P < 0.05$; **, $P < 0.01$; ***, $P < 0.001$; **** P
524 < 0.0001). **E.** Correlation analyses comparing serum neutralizing antibody concentrations three
525 weeks after boosting plotted against lung viral titer (4 dpi) in 129S2 mice after challenge with the
526 indicated SARS-CoV-2 strain (Pearson's correlation P and R^2 values are indicated as insets;
527 closed symbols 5 µg vaccine dose; open symbols, 0.25 µg vaccine dose).

528 **Figure 3. Vaccine-mediated protection against lung pathology in 129S2 mice.**
529 Seven to nine-week-old female 129S2 mice were immunized, boosted with 0.25 µg of mRNA
530 vaccines (control, mRNA-1273, mRNA-1273.351, or mRNA-1273.211), and challenged with
531 B.1.351 as described in **Figure 2.** Hematoxylin and eosin staining of lung sections harvested at
532 4 dpi or from a mock-infected animal. Images show low- (top; scale bars, 1 mm) and high-power
533 (bottom; scale bars, 50 µm). Representative images from n = 2 per group.

534 **Figure 4. Immunogenicity analysis of mRNA vaccines in K18-hACE2 transgenic**
535 **mice.** Seven-week-old female K18-hACE2 mice were immunized and boosted with 5 or 0.25 μ g
536 of mRNA vaccines (control (black symbols), mRNA-1273 (red symbols), or mRNA-1273.351
537 (blue symbols). **A.** Scheme of immunizations, spleen harvest, blood draw, and virus challenge.
538 **B.** Serum anti-spike IgG responses at three weeks after booster immunization with mRNA
539 vaccines (control (black symbols), mRNA-1273 (red symbols), mRNA-1273.351 (blue symbols)
540 against indicated spike proteins (Wuhan-1, B.1.1.7, B.1.351, or B.1.617.2). (n = 3 (control
541 vaccine) or 8 (spike vaccines), two independent experiments, boxes illustrate mean value,
542 dotted line shows the LOD; two-way ANOVA with Tukey's post-test: *, $P < 0.05$; **, $P < 0.01$). **C-**
543 **L.** Serum neutralizing antibody responses three weeks after boosting as judged by FRNT (half-
544 maximal reduction, FRNT₅₀ values) with WA1/2020 D614G (**C, H**), WA1/2020 D614G/N501Y
545 (**D, I**), B.1.1.7/E484K (**E, J**), B.1.351 (**F, K**), or B.1.617.2 (**G, L**) in mice immunized with 5 (**C-G**)
546 or 0.25 (**H-L**) μ g of control (n = 5-10), mRNA-1273 (n = 20-24), and mRNA-1273.351 (n = 21-
547 24) vaccines (two independent experiments, boxes illustrate geometric mean values, dotted line
548 shows LOD; one-way Kruskal-Wallis ANOVA with Dunn's post-test: *, $P < 0.05$; **, $P < 0.01$; ***,
549 $P < 0.001$; **** $P < 0.0001$). **M-N.** Antigenic map of sera from K18-hACE2 mice titrated against
550 WA1/2020 D614G, WA1/2020 N501Y/D614G, B.1.1.7/E484K, B.1.351, and B.1.617.2. The
551 maps show sera from immunized mice that received 5 μ g (**M**) or 0.25 μ g (**N**) doses, respectively
552 with symbol details described in **Figure 1**. **O-R.** CD8⁺ (**O, P**) and CD4⁺ (**Q, R**) T cell responses
553 in K18-hACE2 mice at day 35, two weeks after booster immunization with mRNA vaccines (n=
554 10 for each group, two independent experiments, boxes illustrate median values, one-way
555 ANOVA with Tukey's post-test: ns, not significant; *, $P < 0.05$; **, $P > 0.01$; ***, $P < 0.001$; **** P
556 < 0.0001).

557 **Figure 5. Protection against SARS-CoV-2 infection after mRNA vaccination in K18-**
558 **hACE2 transgenic mice.** Seven-week-old female K18-hACE2 mice were immunized and

559 boosted with 5 or 0.25 μg of mRNA vaccines (control (black symbols), mRNA-1273 (red
560 symbols), or mRNA-1273.351 (blue symbols) as described in **Figure 4A**. Four weeks after
561 boosting, mice were challenged via intranasal inoculation with 10^3 to 3×10^4 FFU of WA1/2020
562 D614G, WA1/2020 N501Y/D614G, B.1.1.7/E484K, B.1.351, or B.1.617.2, depending on the
563 strain. **A-B**. Body weight change over time. Data shown is the mean \pm SEM ($n = 4-8$, two
564 independent experiments; one-way ANOVA of area under the curve from 2-4 dpi with Dunnett's
565 post-test, comparison to control immunized group: **** $P < 0.0001$). **C-D**. Viral burden levels at
566 6 dpi in the nasal washes (**C**) and lungs (**D**) as assessed by qRT-PCR of the *N* gene after
567 challenge of immunized mice with the indicated mRNA vaccines ($n = 4-8$, two independent
568 experiments, boxes illustrate median values, dotted line shows LOD; one-way Kruskal-Wallis
569 ANOVA with Dunn's post-test, comparison among all immunization groups: *, $P < 0.05$; **, $P <$
570 0.01 ; ***, $P < 0.001$; **** $P < 0.0001$). **E**. Correlation analyses comparing serum neutralizing
571 antibody concentrations three weeks after boosting plotted against lung viral titer (6 dpi) in K18-
572 hACE2 mice after challenge with the indicated SARS-CoV-2 strain (Pearson's correlation P and
573 R^2 values are indicated as insets; closed symbols 5 μg vaccine dose; open symbols, 0.25 μg
574 vaccine dose).

575 **Figure 6. High dose mRNA vaccine protection against lung inflammation and**
576 **pathology in K18-hACE2 transgenic mice.** Seven to nine-week-old female K18-hACE2
577 transgenic mice were immunized, boosted with 5 μg of mRNA vaccines (control, mRNA-1273,
578 or mRNA-1273.351, and challenged with WA1/2020, WA1/2020 N501Y/D614G, B.1.1.7/E484K,
579 B.1.351, or B.1.617.2. as described in **Figure 5**. Hematoxylin and eosin staining of lung sections
580 harvested at 6 dpi or from an uninfected animal. Images show low- (top; scale bars, 1 mm) and
581 high-power (bottom; scale bars, 50 μm). Representative images of multiple lung sections from n
582 = 2 per group.

583 **Figure 7. Low dose mRNA vaccine protection against lung inflammation and**
584 **pathology in K18-hACE2 transgenic mice.** Seven to nine-week-old female K18-hACE2
585 transgenic mice were immunized, boosted with 0.25 µg of mRNA vaccines (control, mRNA-
586 1273, or mRNA-1273.351, and challenged with WA1/2020, WA1/2020 N501Y/D614G,
587 B.1.1.7/E484K, B.1.351, or B.1.617.2. as described in **Figure 5**. Hematoxylin and eosin staining
588 of lung sections harvested at 6 dpi or from an uninfected animal. Images show low- (top; scale
589 bars, 1 mm) and high-power (bottom; scale bars, 50 µm). Representative images of multiple
590 lung sections from n = 2 per group.
591

592 **SUPPLEMENTAL FIGURE LEGENDS**

593 **Figure S1. Analysis of serum neutralization of SARS-CoV-2 strains from 129S2**
594 **mice immunized with mRNA vaccines, Related to Figure 1.** Comparison of neutralizing
595 activity of sera against WA1/2020 D614G, WA1/2020 D614G/N501Y, B.1.1.7/E484K, B.1.351,
596 and B.1.617.2. Sera was obtained three weeks after boosting with 5 μg (**A-C**) or 0.25 μg (**D-F**)
597 of mRNA vaccines: mRNA-1273 (**A and D**), mRNA-1273.351 (**B and E**), and mRNA-1273.211
598 (**C and F**). Results are from experiments performed in **Figure 1C-L**. Geometric mean
599 neutralization titers (GMT) are shown above each graph, dotted line represents the LOD. Solid
600 lines connect data points from the same serum sample across strains.

601 **Figure S2. Protection against SARS-CoV-2 infection after mRNA vaccination in**
602 **129S2 mice, Related to Figure 2.** Seven to nine-week-old female 129S2 mice were immunized
603 and boosted with 5 or 0.25 μg of mRNA vaccines as described in **Figure 1A**. Three weeks after
604 boosting, mice were challenged via intranasal inoculation with 10^5 FFU of WA1/2020
605 N501Y/D614G, B.1.1.7/E484K, or B.1.351. **A.** Viral burden at 4 dpi in the spleen as assessed
606 by qRT-PCR of the *N* gene after challenge of immunized mice with the indicated mRNA
607 vaccines ($n = 6-8$, two independent experiments; boxes illustrate median values, dotted line
608 shows LOD; one-way Kruskal-Wallis ANOVA with Dunn's post-test, comparison among all
609 immunization groups: ns, not significant; $P > 0.05$; *, $P < 0.05$; **, $P < 0.01$; ***, $P < 0.001$; **** P
610 < 0.0001). **B.** Correlation analyses comparing serum neutralizing antibody concentrations three
611 weeks after boosting plotted against weight change in 129S2 mice after challenge with the
612 indicated SARS-CoV-2 strain (Pearson's correlation P and R^2 values are indicated as insets;
613 closed symbols, 5 μg vaccine dose; open symbols, 0.25 μg vaccine dose).

614 **Figure S3. Analysis of serum neutralization of SARS-CoV-2 strains from K18-**
615 **hACE2 mice immunized with mRNA vaccines, Related to Figure 4.** Comparison of
616 neutralizing activity of sera against WA1/2020 D614G, WA1/2020 D614G/N501Y,

617 B.1.1.7/E484K, B.1.351, and B.1.617.2. Sera was obtained three weeks after boosting with 5 μ g
618 (A-B) or 0.25 μ g (C-D) mRNA vaccines: mRNA-1273 (A and C) and mRNA-1273.351 (B and
619 D), Results are from experiments performed in **Figure 4C-L**. GMTs are shown above each
620 graph, dotted line represents the LOD. Solid lines connect data points from the same serum
621 sample across strains.

622 **Figure S4. Protection against SARS-CoV-2 infection after mRNA vaccination in**
623 **K18-hACE2 transgenic mice, Related to Figure 5.** Seven-week-old K18-hACE2 mice were
624 immunized and boosted with 5 or 0.25 μ g of mRNA vaccines (control (black symbols), mRNA-
625 1273 (red symbols), or mRNA-1273.351 (blue symbols) as described in **Figure 4A**. Three to
626 four weeks after the last boost, mice were challenged via intranasal inoculation with WA1/2020
627 D614, WA1/2020 N501Y/D614G, B.1.1.7/E484K, B.1.351, or B.1.617.2 as described in **Figure**
628 **5. (A)** Viral burden levels at 6 dpi in the brain as assessed by qRT-PCR of the *N* gene after
629 challenge of immunized mice with the indicated mRNA vaccines (n = 4-8, two independent
630 experiments; boxes illustrate median values, dotted line shows LOD; one-way Kruskal-Wallis
631 ANOVA with Dunn's post-test, comparison among all immunization groups: *, $P < 0.05$; **, $P <$
632 0.01 ; ***, $P < 0.001$; **** $P < 0.0001$). **B.** Correlation analyses comparing serum neutralizing
633 antibody concentrations three weeks after boosting plotted against weight change in K18-
634 hACE2 mice after challenge with the indicated SARS-CoV-2 strain (Pearson's correlation P and
635 R^2 values are indicated as insets; closed symbols, 5 μ g vaccine dose; open symbols, 0.25 μ g
636 vaccine dose).

637 **Figure S5. Cytokine induction in lungs after mRNA vaccination and SARS-CoV-2**
638 **challenge, Related to Figure 5.** Cytokine levels from mice immunized with 5 μ g (A-B) or 0.25
639 μ g (C-D) dose of mRNA vaccines as measured by multiplex platform in lung tissues of SARS-
640 CoV-2-infected mice at 6 dpi. **A and C.** For each cytokine, fold-change was calculated
641 compared to mock-inoculated mice and \log_2 (fold-change) was plotted in the corresponding

642 color-coded heat-map. **B and D.** Cytokine levels as measured by multiplex platform in the lungs
643 of SARS-CoV-2-infected mice after vaccination (n = 7-8 per group, two independent
644 experiments, mean values +/- SEM is shown).

645

646 **STAR METHODS**

647 **RESOURCE AVAILABILITY**

648 **Lead Contact.** Further information and requests for resources and reagents should be
649 directed to and will be fulfilled by the Lead Contact, Michael S. Diamond
650 (diamond@wusm.wustl.edu).

651 **Materials Availability.** All requests for resources and reagents should be directed to
652 and will be fulfilled by the Lead Contact author. This includes mice, antibodies, viruses,
653 vaccines, proteins, and peptides. All reagents will be made available on request after
654 completion of a Materials Transfer Agreement.

655 **Data and code availability.** All data supporting the findings of this study are available
656 within the paper and are available from the corresponding author upon request.

657

658 **EXPERIMENTAL MODEL AND SUBJECT DETAILS**

659 **Cells.** Vero-TMPRSS2 (Zang et al., 2020) and Vero-hACE2-TMPRSS2 (Chen et al.,
660 2021b) cells were cultured at 37°C in Dulbecco's Modified Eagle medium (DMEM)
661 supplemented with 10% fetal bovine serum (FBS), 10 mM HEPES pH 7.3, 1 mM sodium
662 pyruvate, 1x non-essential amino acids, and 100 U/mL of penicillin–streptomycin. Vero-
663 TMPRSS2 cells were supplemented with 5 µg/mL of blasticidin. Vero-hACE2-TMPRSS2 cells
664 were supplemented with 10 µg/mL of puromycin. All cells routinely tested negative for
665 mycoplasma using a PCR-based assay.

666 **Viruses.** The WA1/2020 recombinant strain with substitutions (D614G or
667 N501Y/D614G) were obtained from an infectious cDNA clone of the 2019n-
668 CoV/USA_WA1/2020 strain as described previously (Plante et al., 2020). The B.1.351,
669 B.1.1.7/E484K, and B.1.617.2 isolates were originally obtained from nasopharyngeal isolates.
670 All viruses were passaged once in Vero-TMPRSS2 cells and subjected to next-generation

671 sequencing as described previously (Chen et al., 2021b) to confirm the introduction and stability
672 of substitutions. All virus experiments were performed in an approved biosafety level 3 (BSL-3)
673 facility.

674 **Mice.** Animal studies were carried out in accordance with the recommendations in the
675 Guide for the Care and Use of Laboratory Animals of the National Institutes of Health. The
676 protocols were approved by the Institutional Animal Care and Use Committee at the Washington
677 University School of Medicine (assurance number A3381-01). Virus inoculations were
678 performed under anesthesia that was induced and maintained with ketamine hydrochloride and
679 xylazine, and all efforts were made to minimize animal suffering.

680 Heterozygous K18-hACE2 C57BL/6J mice (strain: 2B6.Cg-Tg(K18-ACE2)2PrImn/J) and
681 129 mice (strain: 129S2/SvPasCrl) were obtained from The Jackson Laboratory and Charles
682 River Laboratories, respectively. Animals were housed in groups and fed standard chow diets.

683 **Pre-clinical vaccine mRNA and lipid nanoparticle production process.** A sequence-
684 optimized mRNA encoding prefusion-stabilized Wuhan-Hu-1 (mRNA-1273) or B.1.351-variant
685 (mRNA-1273.351) SARS-CoV-2 S-2P protein was synthesized *in vitro* using an optimized T7
686 RNA polymerase-mediated transcription reaction with complete replacement of uridine by N1m-
687 pseudouridine (Nelson et al., 2020). The reaction included a DNA template containing the
688 immunogen open-reading frame flanked by 5' untranslated region (UTR) and 3' UTR sequences
689 and was terminated by an encoded polyA tail. After transcription, the cap-1 structure was added
690 to the 5' end using the vaccinia virus capping enzyme (New England Biolabs) and vaccinia
691 virus 2'-O-methyltransferase (New England Biolabs). The mRNA was purified by oligo-dT affinity
692 purification, buffer exchanged by tangential flow filtration into sodium acetate, pH 5.0, sterile
693 filtered, and kept frozen at -20°C until further use.

694 The mRNA was encapsulated in a lipid nanoparticle through a modified ethanol-drop
695 nanoprecipitation process described previously (Hassett et al., 2019). Ionizable, structural,
696 helper, and polyethylene glycol lipids were briefly mixed with mRNA in an acetate buffer, pH 5.0,

697 at a ratio of 2.5:1 (lipid:mRNA). The mixture was neutralized with Tris-HCl, pH 7.5, sucrose was
698 added as a cryoprotectant, and the final solution was sterile-filtered. Vials were filled with
699 formulated lipid nanoparticle and stored frozen at -20°C until further use. The vaccine product
700 underwent analytical characterization, which included the determination of particle size and
701 polydispersity, encapsulation, mRNA purity, double-stranded RNA content, osmolality, pH,
702 endotoxin, and bioburden, and the material was deemed acceptable for *in vivo* study.

703 **Antigens.** Recombinant soluble S proteins from different SARS-CoV-2 strains were
704 expressed as previously described (Amanat et al., 2021; Stadlbauer et al., 2020). Briefly,
705 mammalian cell codon-optimized nucleotide sequences coding for the soluble ectodomain of the
706 S protein of SARS-CoV-2 including a C-terminal thrombin cleavage site, T4 foldon trimerization
707 domain, and hexahistidine tag were cloned into mammalian expression vector pCAGGS. The
708 spike protein sequence was modified to remove the polybasic cleavage site (RRAR to A), and
709 two pre-fusion stabilizing proline mutations were introduced (K986P and V987P, wild type
710 Wuhan-Hu-1 numbering). Recombinant proteins were produced in Expi293F cells
711 (ThermoFisher) by transfection with purified DNA using the ExpiFectamine 293 Transfection Kit
712 (ThermoFisher). Supernatants from transfected cells were harvested 3 days post-transfection,
713 and recombinant proteins were purified using Ni-NTA agarose (ThermoFisher), then buffer
714 exchanged into PBS and concentrated using Amicon Ultracel centrifugal filters (EMD Millipore).

715

716 **METHOD DETAILS**

717 **ELISA.** Assays were performed in 96-well microtiter plates (Thermo Fisher) coated with
718 50 μL of recombinant spike from wild type SARS-CoV-2 or variant viruses B.1.1.7, B.1.351, or
719 B.1.617.2. Plates were incubated at 4°C overnight and then blocked with 200 μL of 3% non-fat
720 dry milk (AmericanBio) in PBS containing 0.1% Tween-20 (PBST) for one hour at room
721 temperature (RT). Sera were serially diluted in 1% non-fat dry milk in PBST and added to the
722 plates. Plates were incubated for 120 min at room temperature and then washed 3 times with

723 PBST. Goat anti-mouse IgG-HRP (Sigma-Aldrich, 1:9000) was diluted in 1% non-fat dry milk in
724 PBST before adding to the wells and incubating for 60 min at room temperature. Plates were
725 washed 3 times with PBST before the addition of peroxidase substrate (SigmaFAST o-
726 phenylenediamine dihydrochloride, Sigma-Aldrich). Reactions were stopped by the addition of 3
727 M hydrochloric acid. Optical density (OD) measurements were taken at 490 nm, and endpoint
728 titers were calculated in excel using a 0.15 OD 490 nm cutoff. Graphs were generated using
729 Graphpad Prism v9.

730 **Focus reduction neutralization test.** Serial dilutions of sera were incubated with 10^2
731 focus-forming units (FFU) of different strains of SARS-CoV-2 for 1 h at 37°C. Antibody-virus
732 complexes were added to Vero-TMPRSS2 cell monolayers in 96-well plates and incubated at
733 37°C for 1 h. Subsequently, cells were overlaid with 1% (w/v) methylcellulose in MEM. Plates
734 were harvested 30 h later by removing overlays and fixed with 4% PFA in PBS for 20 min at
735 room temperature. Plates were washed and sequentially incubated with an oligoclonal pool of
736 SARS2-2, SARS2-11, SARS2-16, SARS2-31, SARS2-38, SARS2-57, and SARS2-71 (Liu et al.,
737 2021c) anti-S antibodies and HRP-conjugated goat anti-mouse IgG (Sigma, 12-349) in PBS
738 supplemented with 0.1% saponin and 0.1% bovine serum albumin. SARS-CoV-2-infected cell
739 foci were visualized using TrueBlue peroxidase substrate (KPL) and quantitated on an
740 ImmunoSpot microanalyzer (Cellular Technologies).

741 **Mouse experiments.** Female 129S2 (catalog 287) and K18-hACE2 C57BL/6 (catalog
742 034860) mice were purchased from the Charles River and The Jackson Laboratory,
743 respectively. Seven to nine-week-old animals were immunized and boosted three weeks apart
744 with 0.25 or 5 µg of mRNA vaccines (control, mRNA-1273, mRNA-1273.351, or mRNA-
745 1273.211) in 50 µl PBS via intramuscular injection in the hind leg. Animals were bled at
746 specified time points via the mandibular vein to obtain sera for immunogenicity analysis. Three
747 to four weeks after boosting, mice were inoculated with 10^5 FFU (129S2) or 10^3 to 3×10^4 FFU
748 (K18-hACE2) of WA1/2020 D614G (10^4), WA1/2020 N501Y/D614G (10^3), B.1.1.7/E484K (10^3),

749 B.1.351 (10^3), or B.1.617.2 (3×10^4) of SARS-CoV-2 strains by the intranasal route. Different
750 doses of viruses were used in K18-hACE2 mice to match weight loss and infection in the nasal
751 wash and lungs. This approach was necessary as some viruses (WA1/2020 N501Y/D614G,
752 B.1.1.7/E484K, and B.1.351) encode N501Y mutations that enhance pathogenicity in mice (Gu
753 et al., 2020; Muruato et al., 2021; Rathnasinghe et al., 2021). Animals were euthanized at 4 or 6
754 dpi, and tissues were harvested for virological, immunological, and pathological analyses.

755 **Measurement of viral burden.** Tissues were weighed and homogenized with zirconia
756 beads in a MagNA Lyser instrument (Roche Life Science) in 1000 μ L of DMEM medium
757 supplemented with 2% heat-inactivated FBS. Tissue homogenates were clarified by
758 centrifugation at 10,000 rpm for 5 min and stored at -80°C . RNA was extracted using the
759 MagMax mirVana Total RNA isolation kit (Thermo Fisher Scientific) on the Kingfisher Flex
760 extraction robot (Thermo Fisher Scientific). RNA was reverse transcribed and amplified using
761 the TaqMan RNA-to-CT 1-Step Kit (Thermo Fisher Scientific). Reverse transcription was carried
762 out at 48°C for 15 min followed by 2 min at 95°C . Amplification was accomplished over 50
763 cycles as follows: 95°C for 15 s and 60°C for 1 min. Copies of SARS-CoV-2 *N* gene RNA in
764 samples were determined using a previously published assay (Case et al., 2020a). Briefly, a
765 TaqMan assay was designed to target a highly conserved region of the *N* gene (Forward primer:
766 ATGCTGCAATCGTGCTACAA; Reverse primer: GACTGCCGCCTCTGCTC; Probe: /56-
767 FAM/TCAAGGAAC/ZEN/AACATTGCCAA/3IABkFQ/). This region was included in an RNA
768 standard to allow for copy number determination down to 10 copies per reaction. The reaction
769 mixture contained final concentrations of primers and probe of 500 and 100 nM, respectively.

770 **Cytokine and chemokine protein measurements.** Lung homogenates were incubated
771 with Triton-X-100 (1% final concentration) for 1 h at room temperature to inactivate SARS-CoV-
772 2. Homogenates then were analyzed for cytokines and chemokines by Eve Technologies
773 Corporation (Calgary, AB, Canada) using their Mouse Cytokine Array/Chemokine Array 31-Plex
774 (MD31) platform.

775 **Lung histology.** Animals were euthanized before harvest and fixation of tissues. Lungs
776 were inflated with ~2 mL of 10% neutral buffered formalin using a 3-mL syringe and catheter
777 inserted into the trachea and kept in fixative for 7 days. Tissues were embedded in paraffin, and
778 sections were stained with hematoxylin and eosin. Images were captured using the
779 Nanozoomer (Hamamatsu) at the Alafi Neuroimaging Core at Washington University.

780 **Peptide restimulation and intracellular cytokine staining.** Two weeks after boosting,
781 splenocytes from vaccinated K18-hACE2 mice were stimulated *ex vivo* with an H-2D^b-restricted
782 CD8 or CD4 immunodominant peptide (amino acids 262–270 and 62-76 of the S protein,
783 respectively; gift of K. Valentine and S. Shresta, La Jolla Institute for Immunology) for 16 h at
784 37°C with brefeldin A (BioLegend, 420601) added for the last 4 h of incubation. Following
785 blocking with FcγR antibody (BioLegend, clone 93), cells were stained on ice with CD45
786 BUV395 (BD BioSciences clone 30-F11), CD4 PE (BD BioSciences clone GK1.5), CD8 FITC
787 (BioLegend clone 53-6.7), and Fixable Aqua Dead Cell Stain (Invitrogen, L34966). Stained cells
788 were fixed and permeabilized with the Foxp3/Transcription Factor Staining Buffer Set
789 (eBiosciences, 00-5523). Subsequently, intracellular staining was performed with anti-IFN-γ
790 Alexa 647 (BioLegend, clone XMG1.2), and anti-TNFα BV605 (BioLegend, clone MP6-XT22).
791 Analysis was performed on a BD LSRFortessa X-20 cytometer, using FlowJo X 10.0 software.

792 **Antigenic cartography.** A target distance from an individual serum to each virus was
793 derived by calculating the difference between the logarithm (log₂) reciprocal neutralization titer
794 for that particular virus and the log₂ reciprocal maximum titer achieved by that serum (against
795 any virus). Thus, the higher the reciprocal titer, the shorter the target distance. As the log₂ of the
796 reciprocal titer was used, a 2-fold change in titer equates to a fixed change in target distance
797 whatever the magnitude of the actual titers. Antigenic cartography (Smith et al., 2004) then was
798 used to optimize the positions of the viruses and sera relative to each other on a map,
799 minimizing the sum-squared error between map distance and target distance. Each virus is

800 therefore positioned by multiple sera, and the sera themselves also are positioned only by their
801 distances to the viruses. Hence, sera with different neutralization profiles to the virus panel are
802 in separate locations on the map but contribute equally to positioning of the viruses.

803

804 **QUANTIFICATION AND STATISTICAL ANALYSIS**

805 Statistical significance was assigned when P values were < 0.05 using Prism Version 10
806 (GraphPad). Tests, number of animals (n), median values, and statistical comparison groups
807 are indicated in the Figure legends.

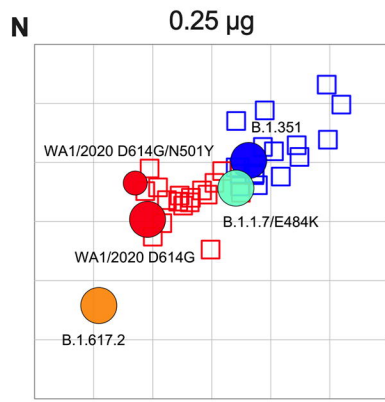
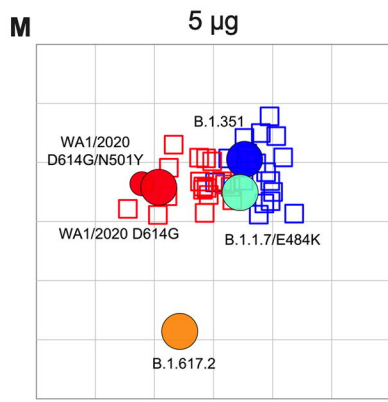
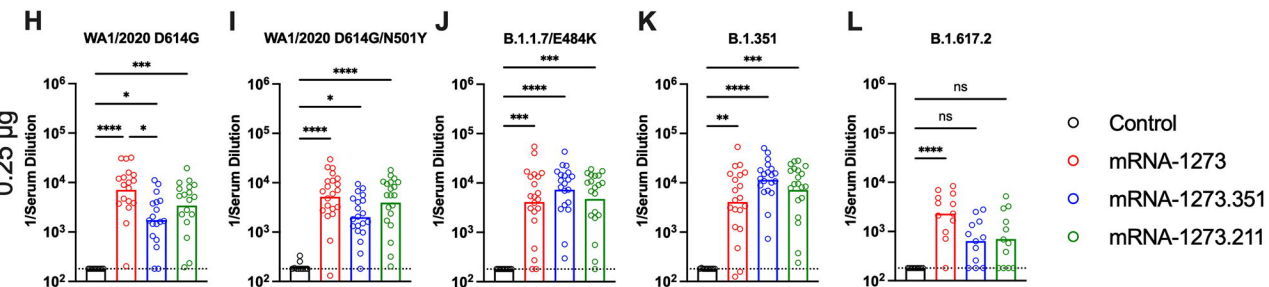
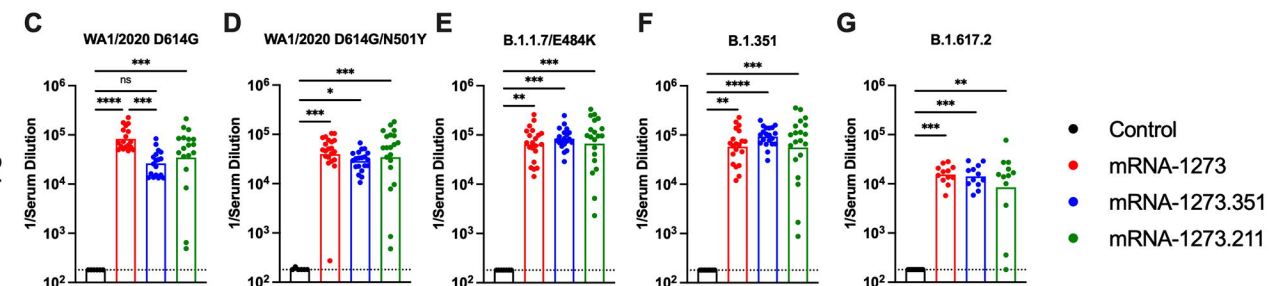
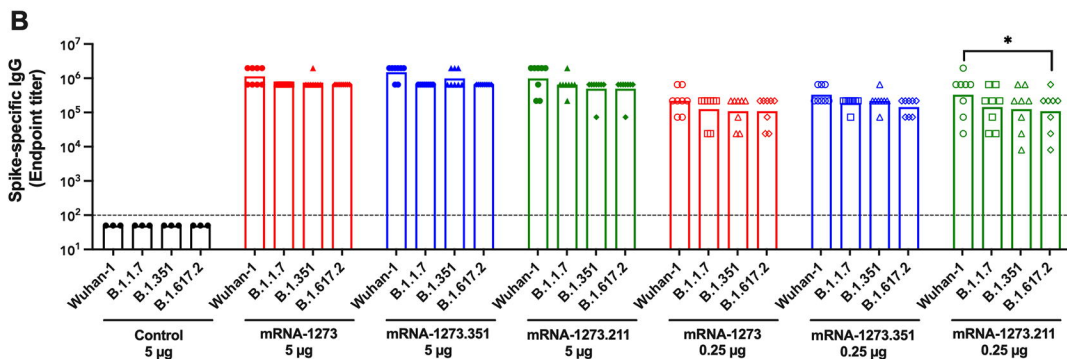
808 **REFERENCES**

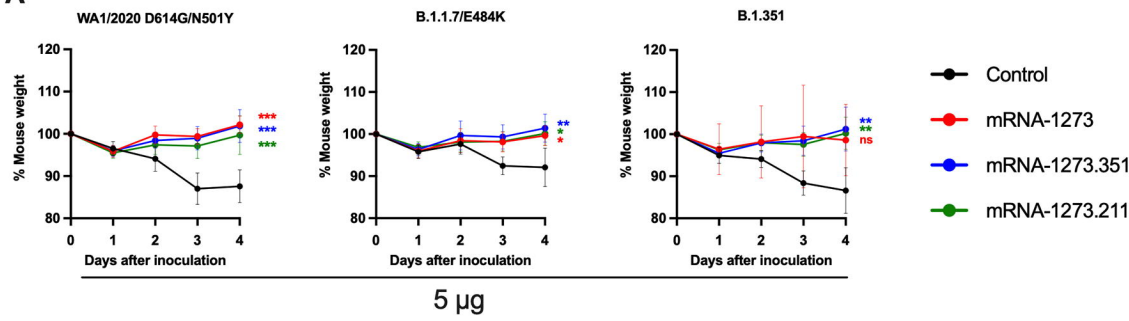
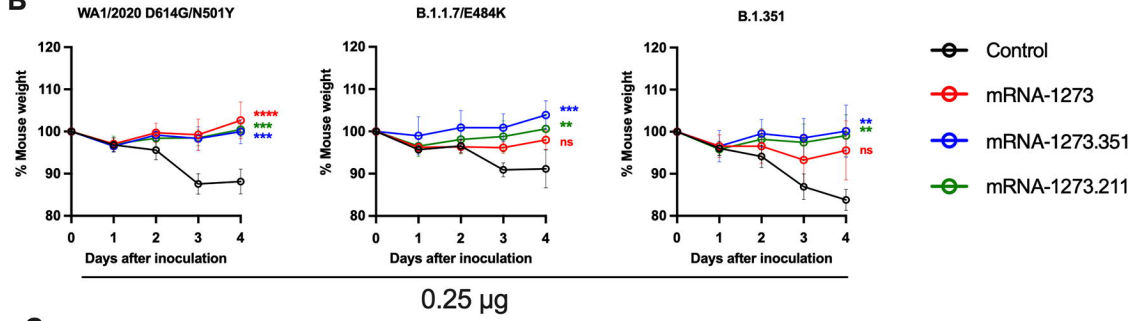
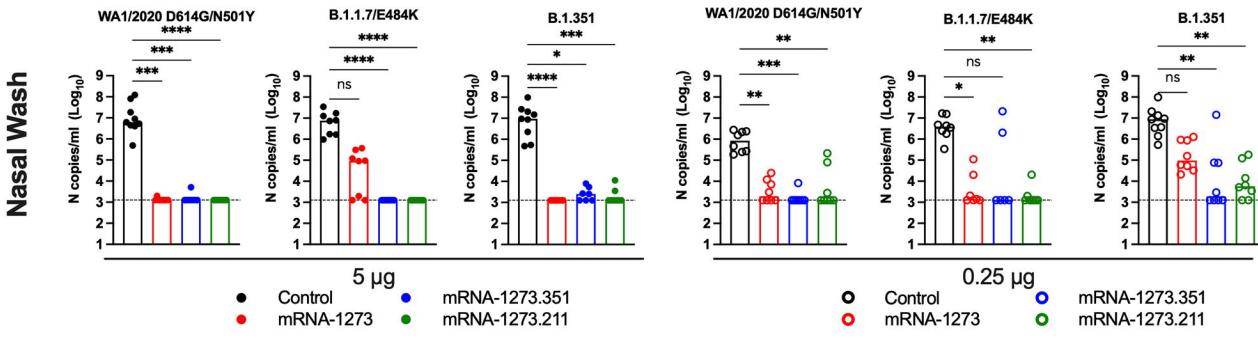
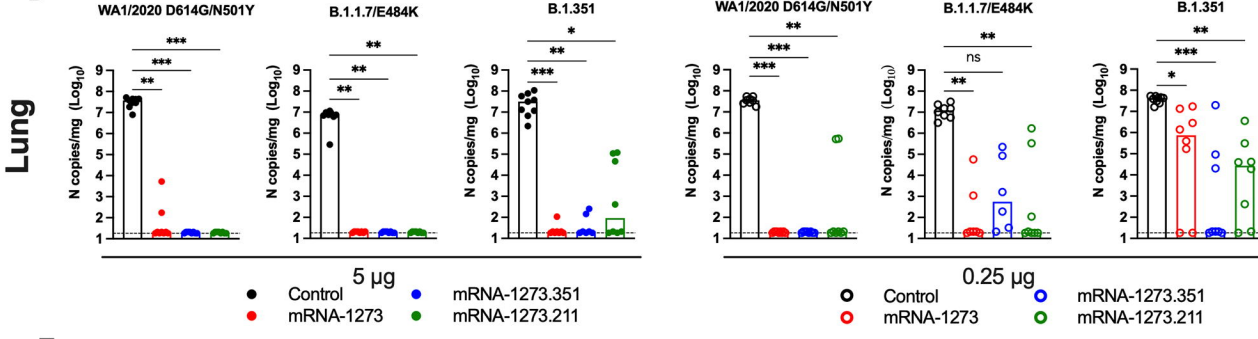
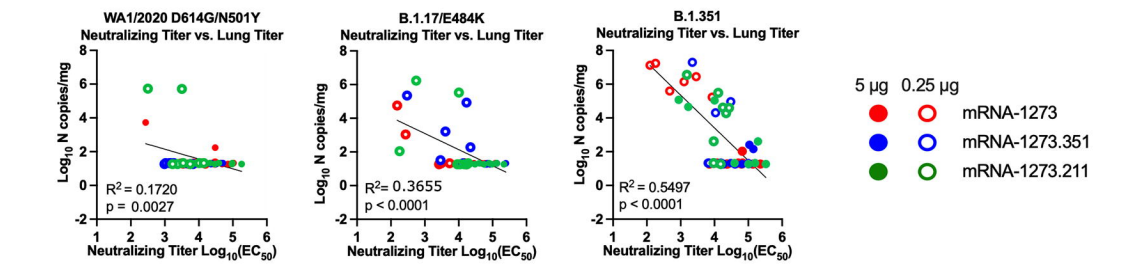
- 809 Abu-Raddad, L.J., Chemaitelly, H., and Butt, A.A. (2021). Effectiveness of the BNT162b2 Covid-
810 19 Vaccine against the B.1.1.7 and B.1.351 Variants. *N Engl J Med*.
811
812 Amanat, F., Thapa, M., Lei, T., Ahmed, S.M.S., Adelsberg, D.C., Carreño, J.M., Strohmeier, S.,
813 Schmitz, A.J., Zafar, S., Zhou, J.Q., *et al.* (2021). SARS-CoV-2 mRNA vaccination induces
814 functionally diverse antibodies to NTD, RBD, and S2. *Cell* *184*, 3936-3948.e3910.
815
816 Baden, L.R., El Sahly, H.M., Essink, B., Kotloff, K., Frey, S., Novak, R., Diemert, D., Spector,
817 S.A., Roupheal, N., Creech, C.B., *et al.* (2021). Efficacy and Safety of the mRNA-1273 SARS-
818 CoV-2 Vaccine. *N Engl J Med* *385*, 403-416.
819
820 Brown, C.M., Vostok, J., Johnson, H., Burns, M., Gharpure, R., Sami, S., Sabo, R.T., Hall, N.,
821 Foreman, A., Schubert, P.L., *et al.* (2021). Outbreak of SARS-CoV-2 Infections, Including
822 COVID-19 Vaccine Breakthrough Infections, Associated with Large Public Gatherings -
823 Barnstable County, Massachusetts, July 2021. *MMWR Morb Mortal Wkly Rep* *70*, 1059-1062.
824
825 Case, J.B., Bailey, A.L., Kim, A.S., Chen, R.E., and Diamond, M.S. (2020a). Growth, detection,
826 quantification, and inactivation of SARS-CoV-2. *Virology* *548*, 39-48.
827
828 Case, J.B., Rothlauf, P.W., Chen, R.E., Liu, Z., Zhao, H., Kim, A., S., Bloyet, L.M., Zeng, Q.,
829 Tahan, S., Droit, L., *et al.* (2020b). Neutralizing antibody and soluble ACE2 inhibition of a
830 replication-competent VSV-SARS-CoV-2 and a clinical isolate of SARS-CoV-2. *Cell Host and*
831 *Microbe* *28*, 475-485.
832
833 Chen, R.E., Winkler, E.S., Case, J.B., Aziati, I.D., Bricker, T.L., Joshi, A., Darling, T.L., Ying, B.,
834 Errico, J.M., Shrihari, S., *et al.* (2021a). In vivo monoclonal antibody efficacy against SARS-
835 CoV-2 variant strains. *Nature*.
836
837 Chen, R.E., Zhang, X., Case, J.B., Winkler, E.S., Liu, Y., VanBlargan, L.A., Liu, J., Errico, J.M.,
838 Xie, X., Suryadevara, N., *et al.* (2021b). Resistance of SARS-CoV-2 variants to neutralization by
839 monoclonal and serum-derived polyclonal antibodies. *Nat Med*.
840
841 Corbett, K.S., Werner, A.P., Connell, S.O., Gagne, M., Lai, L., Moliva, J.I., Flynn, B., Choi, A.,
842 Koch, M., Foulds, K.E., *et al.* (2021). mRNA-1273 protects against SARS-CoV-2 beta infection
843 in nonhuman primates. *Nat Immunol*.
844
845 Graham, B.S. (2020). Rapid COVID-19 vaccine development. *Science* *368*, 945-946.
846
847 Gu, H., Chen, Q., Yang, G., He, L., Fan, H., Deng, Y.Q., Wang, Y., Teng, Y., Zhao, Z., Cui, Y.,
848 *et al.* (2020). Adaptation of SARS-CoV-2 in BALB/c mice for testing vaccine efficacy. *Science*
849 *369*, 1603-1607.
850
851 Hassett, K.J., Benenato, K.E., Jacquinet, E., Lee, A., Woods, A., Yuzhakov, O., Himansu, S.,
852 Deterling, J., Geilich, B.M., Ketova, T., *et al.* (2019). Optimization of Lipid Nanoparticles for
853 Intramuscular Administration of mRNA Vaccines. *Molecular therapy Nucleic acids* *15*, 1-11.
854
855 Ibarondo, F.J., Hofmann, C., Fulcher, J.A., Goodman-Meza, D., Mu, W., Hausner, M.A., Ali, A.,
856 Balamurugan, A., Taus, E., Elliott, J., *et al.* (2021). Primary, Recall, and Decay Kinetics of
857 SARS-CoV-2 Vaccine Antibody Responses. *ACS Nano*.

858
859 Krause, P.R., Fleming, T.R., Longini, I.M., Peto, R., Briand, S., Heymann, D.L., Beral, V.,
860 Snape, M.D., Rees, H., Ropero, A.M., *et al.* (2021). SARS-CoV-2 Variants and Vaccines. *N*
861 *Engl J Med* 385, 179-186.
862
863 Kruglova, N., Siniavin, A., Gushchin, V., and Mazurov, D. (2021). Different Neutralization
864 Sensitivity of SARS-CoV-2 Cell-to-Cell and Cell-Free Modes of Infection to Convalescent Sera.
865 *Viruses* 13.
866
867 Liu, C., Ginn, H.M., Dejnirattisai, W., Supasa, P., Wang, B., Tuekprakhon, A., Nutalai, R., Zhou,
868 D., Mentzer, A.J., Zhao, Y., *et al.* (2021a). Reduced neutralization of SARS-CoV-2 B.1.617 by
869 vaccine and convalescent serum. *Cell* 184, 4220-4236.e4213.
870
871 Liu, Y., Hu, G., Wang, Y., Ren, W., Zhao, X., Ji, F., Zhu, Y., Feng, F., Gong, M., Ju, X., *et al.*
872 (2021b). Functional and genetic analysis of viral receptor ACE2 orthologs reveals a broad
873 potential host range of SARS-CoV-2. *Proc Natl Acad Sci U S A* 118.
874
875 Liu, Z., VanBlargan, L.A., Bloyet, L.M., Rothlauf, P.W., Chen, R.E., Stumpf, S., Zhao, H., Errico,
876 J.M., Theel, E.S., Liebeskind, M.J., *et al.* (2021c). Identification of SARS-CoV-2 spike mutations
877 that attenuate monoclonal and serum antibody neutralization. *Cell Host Microbe* 29, 477-
878 488.e474.
879
880 Madhi, S.A., Baillie, V., Cutland, C.L., Voysey, M., Koen, A.L., Fairlie, L., Padayachee, S.D.,
881 Dheda, K., Barnabas, S.L., Borat, Q.E., *et al.* (2021). Efficacy of the ChAdOx1 nCoV-19 Covid-
882 19 Vaccine against the B.1.351 Variant. *N Engl J Med* 384, 1885-1898.
883
884 Mateus, J., Dan, J.M., Zhang, Z., Moderbacher, C.R., Lammers, M., Goodwin, B., Sette, A.,
885 Crotty, S., and Weiskopf, D. (2021). Low dose mRNA-1273 COVID-19 vaccine generates
886 durable T cell memory and antibodies enhanced by pre-existing crossreactive T cell memory.
887 *medRxiv*.
888
889 McCallum, M., Bassi, J., Marco, A., Chen, A., Walls, A.C., Julio, J.D., Tortorici, M.A., Navarro,
890 M.J., Silacci-Fregni, C., Saliba, C., *et al.* (2021a). SARS-CoV-2 immune evasion by variant
891 B.1.427/B.1.429. *bioRxiv*.
892
893 McCallum, M., Walls, A.C., Sprouse, K.R., Bowen, J.E., Rosen, L., Dang, H.V., deMarco, A.,
894 Franko, N., Tilles, S.W., Logue, J., *et al.* (2021b). Molecular basis of immune evasion by the
895 delta and kappa SARS-CoV-2 variants. *bioRxiv*.
896
897 Muñoz-Fontela, C., Dowling, W.E., Funnell, S.G.P., Gsell, P.S., Riveros-Balta, A.X., Albrecht,
898 R.A., Andersen, H., Baric, R.S., Carroll, M.W., Cavaleri, M., *et al.* (2020). Animal models for
899 COVID-19. *Nature* 586, 509-515.
900
901 Muruato, A., Vu, M.N., Johnson, B.A., Davis-Gardner, M.E., Vanderheiden, A., Lokugmage, K.,
902 Schindewolf, C., Crocquet-Valdes, P.A., Langsjoen, R.M., Plante, J.A., *et al.* (2021). Mouse
903 Adapted SARS-CoV-2 protects animals from lethal SARS-CoV challenge. *bioRxiv*.
904
905 Nelson, J., Sorensen, E.W., Mintri, S., Rabideau, A.E., Zheng, W., Besin, G., Khatwani, N., Su,
906 S.V., Miracco, E.J., Issa, W.J., *et al.* (2020). Impact of mRNA chemistry and manufacturing
907 process on innate immune activation. *Science advances* 6, eaaz6893.
908

909 Pegu, A., O'Connell, S., Schmidt, S.D., O'Dell, S., Talana, C.A., Lai, L., Albert, J., Anderson, E.,
910 Bennett, H., Corbett, K.S., *et al.* (2021). Durability of mRNA-1273 vaccine-induced antibodies
911 against SARS-CoV-2 variants. *Science*.
912
913 Plante, J.A., Liu, Y., Liu, J., Xia, H., Johnson, B.A., Lokugamage, K.G., Zhang, X., Muruato,
914 A.E., Zou, J., Fontes-Garfias, C.R., *et al.* (2020). Spike mutation D614G alters SARS-CoV-2
915 fitness. *Nature*.
916
917 Puranik, A., Lenehan, P.J., Silvert, E., Niesen, M.J.M., Corchado-Garcia, J., JC, O.H., Virk, A.,
918 Swift, M.D., Halamka, J., Badley, A.D., *et al.* (2021). Comparison of two highly-effective mRNA
919 vaccines for COVID-19 during periods of Alpha and Delta variant prevalence. *medRxiv*.
920
921 Rathnasinghe, R., Jangra, S., Cupic, A., Martínez-Romero, C., Mulder, L.C.F., Kehrer, T., Yildiz,
922 S., Choi, A., Mena, I., De Vrieze, J., *et al.* (2021). The N501Y mutation in SARS-CoV-2 spike
923 leads to morbidity in obese and aged mice and is neutralized by convalescent and post-
924 vaccination human sera. *medRxiv*.
925
926 Ravetch, J., Yamin, R., Jones, A., Hoffmann, H.H., Kao, K., Francis, R., Sheahan, T., Baric, R.,
927 Rice, C., and Bournazos, S. (2021). Fc-engineered antibody therapeutics with improved efficacy
928 against COVID-19. *Research square*.
929
930 Sadoff, J., Gray, G., Vandebosch, A., Cárdenas, V., Shukarev, G., Grinsztejn, B., Goepfert,
931 P.A., Truyers, C., Fennema, H., Spiessens, B., *et al.* (2021). Safety and Efficacy of Single-Dose
932 Ad26.COV2.S Vaccine against Covid-19. *N Engl J Med* 384, 2187-2201.
933
934 Shinde, V., Bhikha, S., Hoosain, Z., Archary, M., Bhorat, Q., Fairlie, L., Lalloo, U., Masilela,
935 M.S.L., Moodley, D., Hanley, S., *et al.* (2021). Efficacy of NVX-CoV2373 Covid-19 Vaccine
936 against the B.1.351 Variant. *N Engl J Med* 384, 1899-1909.
937
938 Smith, D.J., Lapedes, A.S., de Jong, J.C., Bestebroer, T.M., Rimmelzwaan, G.F., Osterhaus,
939 A.D., and Fouchier, R.A. (2004). Mapping the antigenic and genetic evolution of influenza virus.
940 *Science* 305, 371-376.
941
942 Stadlbauer, D., Amanat, F., Chromikova, V., Jiang, K., Strohmeier, S., Arunkumar, G.A., Tan, J.,
943 Bhavsar, D., Capuano, C., Kirkpatrick, E., *et al.* (2020). SARS-CoV-2 Seroconversion in
944 Humans: A Detailed Protocol for a Serological Assay, Antigen Production, and Test Setup. *Curr*
945 *Protoc Microbiol* 57, e100.
946
947 Tada, T., Dcosta, B.M., Samanovic-Golden, M., Herati, R.S., Cornelius, A., Mulligan, M.J., and
948 Landau, N.R. (2021). Neutralization of viruses with European, South African, and United States
949 SARS-CoV-2 variant spike proteins by convalescent sera and BNT162b2 mRNA vaccine-
950 elicited antibodies. *bioRxiv*.
951
952 Wang, P., Nair, M.S., Liu, L., Iketani, S., Luo, Y., Guo, Y., Wang, M., Yu, J., Zhang, B., Kwong,
953 P.D., *et al.* (2021a). Antibody Resistance of SARS-CoV-2 Variants B.1.351 and B.1.1.7. *Nature*.
954 Wang, Z., Schmidt, F., Weisblum, Y., Muecksch, F., Barnes, C.O., Finkin, S., Schaefer-
955 Babajew, D., Cipolla, M., Gaebler, C., Lieberman, J.A., *et al.* (2021b). mRNA vaccine-elicited
956 antibodies to SARS-CoV-2 and circulating variants. *Nature*.
957

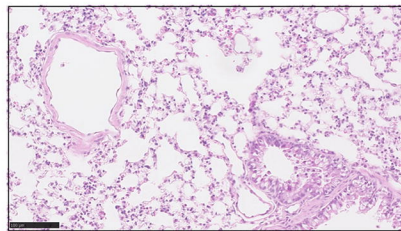
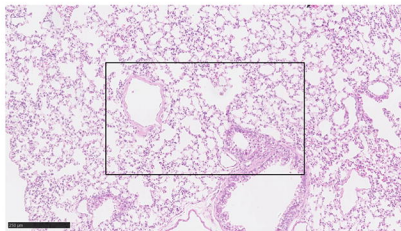
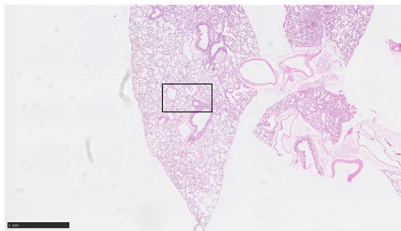
- 958 Wibmer, C.K., Ayres, F., Hermanus, T., Madzivhandila, M., Kgagudi, P., Lambson, B.E.,
959 Vermeulen, M., van den Berg, K., Rossouw, T., Boswell, M., *et al.* (2021). SARS-CoV-2
960 501Y.V2 escapes neutralization by South African COVID-19 donor plasma. *bioRxiv*.
961
- 962 Winkler, E.S., Bailey, A.L., Kafai, N.M., Nair, S., McCune, B.T., Yu, J., Fox, J.M., Chen, R.E.,
963 Earnest, J.T., Keeler, S.P., *et al.* (2020). SARS-CoV-2 infection of human ACE2-transgenic
964 mice causes severe lung inflammation and impaired function. *Nat Immunol* *21*, 1327-1335.
965
- 966 Winkler, E.S., Gilchuk, P., Yu, J., Bailey, A.L., Chen, R.E., Chong, Z., Zost, S.J., Jang, H.,
967 Huang, Y., Allen, J.D., *et al.* (2021). Human neutralizing antibodies against SARS-CoV-2 require
968 intact Fc effector functions for optimal therapeutic protection. *Cell* *184*, 1804-1820.e1816.
969
- 970 Wu, K., Choi, A., Koch, M., Elbashir, S., Ma, L., Lee, D., Woods, A., Henry, C., Palandjian, C.,
971 Hill, A., *et al.* (2021). Variant SARS-CoV-2 mRNA vaccines confer broad neutralization as
972 primary or booster series in mice. *bioRxiv*.
973
- 974 Zang, R., Gomez Castro, M.F., McCune, B.T., Zeng, Q., Rothlauf, P.W., Sonnek, N.M., Liu, Z.,
975 Brulois, K.F., Wang, X., Greenberg, H.B., *et al.* (2020). TMPRSS2 and TMPRSS4 promote
976 SARS-CoV-2 infection of human small intestinal enterocytes. *Sci Immunol* *5*.
977



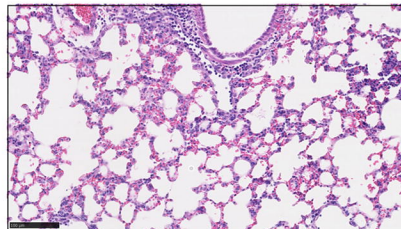
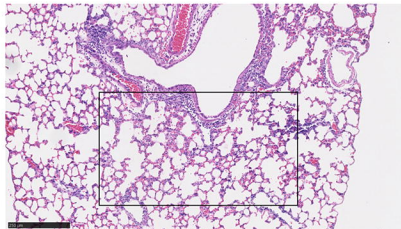
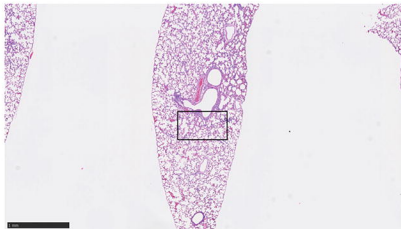
A**B****C****D****E**

0.25 μ g

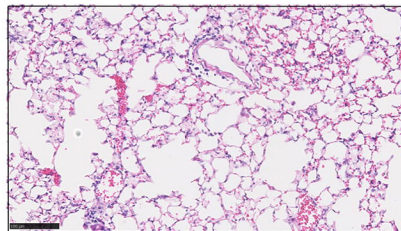
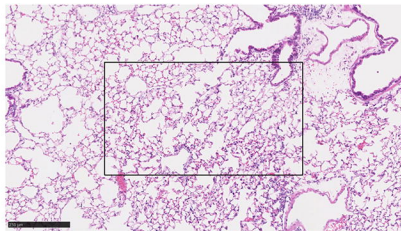
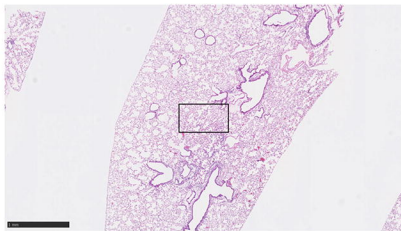
naive



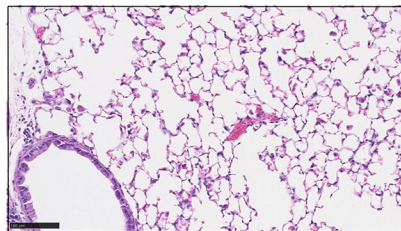
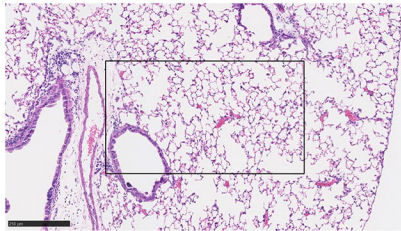
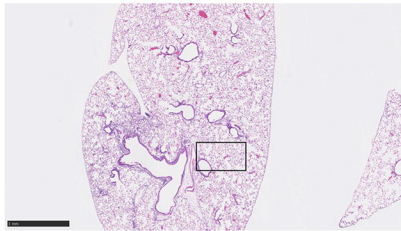
Control



mRNA-1273



mRNA-1273.351



mRNA-1273.211

